Published in final edited form as:
J Am Chem Soc. 2009 August 26; 131(33): 11985–11997. doi:10.1021/ja904400d.

Nitroxyl Radical plus Hydroxylamine Pseudo Self-Exchange Reactions: Tunneling in Hydrogen Atom Transfer

Adam Wu[§], **Elizabeth A. Mader**[§], **Ayan Datta**[†], **David A. Hrovat**[†], **Weston Thatcher Borden**[†], and **James M. Mayer**[§]
Department of Chemistry, Campus Box 351700, University of Washington, Seattle, WA, 98195−1700, USA and Department of Chemistry, P.O. Box 305070, University of North Texas, Denton, TX 76203−5070 USA

Abstract

Bimolecular rate constants have been measured for reactions that involve hydrogen atom transfer (HAT) from hydroxylamines to nitroxyl radicals, using the stable radicals TEMPO$^{\bullet}$ (2,2,6,6-tetramethylpiperidine-1-oxyl radical), 4-oxo-TEMPO$^{\bullet}$ (2,2,6,6-tetramethyl-4-oxo-piperidine-1-oxyl radical), di-*tert*-butylnitroxyl ($^{t}Bu_2NO^{\bullet}$), and the hydroxylamines TEMPO-H, 4-oxo-TEMPO-H, 4-MeO-TEMPO-H (2,2,6,6-tetramethyl-*N*-hydroxy-4-methoxy-piperidine), and $^{t}Bu_2NOH$. The reactions have been monitored by UV-vis stopped-flow methods, using the different optical spectra of nitroxyl radicals. The HAT reactions all have $|\Delta G^{o}| \leq 1.4$ kcal mol^{-1} and therefore are close to self-exchange reactions. The reaction of 4-oxo-TEMPO$^{\bullet}$ + TEMPO-H → 4-oxo-TEMPO-H + TEMPO$^{\bullet}$ occurs with $k_{2H,MeCN} = 10 \pm 1$ M^{-1} s^{-1} in MeCN at 298 K ($K_{2H,MeCN} = 4.5 \pm 1.8$). Surprisingly, the rate constant for the analogous deuterium atom transfer reaction is much slower: $k_{2D,MeCN} = 0.44 \pm 0.05$ M^{-1} s^{-1} with $k_{2H,MeCN}/k_{2D,MeCN} = 23 \pm 3$ at 298 K. The same large kinetic isotope effect (KIE) is found in CH_2Cl_2, 23 ± 4, suggesting that the large KIE is not caused by solvent dynamics or hydrogen bonding to solvent. The related reaction of 4-oxo-TEMPO$^{\bullet}$ with 4-MeO-TEMPO-H(D) also has a large KIE, $k_{3H}/k_{3D} = 21 \pm 3$ in MeCN. For these three reactions, the $E_{aD} - E_{aH}$ values, between 0.3 ± 0.6 and 1.3 ± 0.6 kcal mol^{-1}, and the log(A_H/A_D) values, between 0.5 ± 0.7 and 1.1 ± 0.6, indicate that hydrogen tunneling plays an important role. The related reaction of $^{t}Bu_2NO^{\bullet}$ + TEMPO-H(D) in MeCN has a large KIE, 16 ± 3 in MeCN, and very unusual isotopic activation parameters, $E_{aD} - E_{aH} = -2.6 \pm 0.4$ and log(A_H/A_D) = 3.1 ± 0.6. Computational studies, using POLYRATE, also indicate substantial tunneling in the $(CH_3)_2NO^{\bullet}$ + $(CH_3)_2NOH$ model reaction for the experimental self-exchange processes. Additional calculations on TEMPO($^{\bullet}$/H), $^{t}Bu_2NO$($^{\bullet}$/H), and Ph_2NO($^{\bullet}$/H) self-exchange reactions reveal why the phenyl groups make the last of these reactions several orders of magnitude faster than the first two. By inference, the calculations also suggest why tunneling appears to be more important in the self-exchange reactions of dialkylhydroxylamines than of arylhydroxylamines.

Introduction

Hydrogen transfer reactions are among the most fundamental of chemical reactions.[1] Tunneling of the proton is emphasized in many treatments of hydrogen transfer,[1 2 3-4] and an

E-mail: borden@unt.edu; mayer@chem.washington.edu.
[§]University of Washington.
[†]University of North Texas.

Supporting Information **Available:** Figures S1-S3, the complete author lists for references 32 and 33, the optimized geometries, energies, frequencies and thermal corrections for nitroxyl radicals (RR′NO.), hydroxylamines (RR'NOH), the corresponding hydrogen bonded complexes and hydrogen atom transfer transition structures, for R = R′ = Me, R = H/R′ = Me, R = R′ = ^{t}butyl, R = R′ = phenyl, and TEMPO (34 pages). This material is available free of charge via the Internet at http://pubs.acs.org.

increasing number of these reactions are being found to have large hydrogen/deuterium kinetic isotope effects (KIEs) and activation parameters that indicate the importance of tunneling.[5] While a number of these reactions are understood in detail, there is limited intuition about why some hydrogen-transfer reactions display the hallmarks of tunneling and others do not. Described here are experimental and computational studies of hydrogen-atom transfer (HAT) pseudo self-exchange reactions between dialkylnitroxyl radicals and dialkylhydroxylamines (eq 1) that indicate the occurrence of substantial hydrogen tunneling. These are simple and unusual cases of tunneling in oxygen-to-oxygen HAT. The contrast between these reactions and the closely related reactions of arylnitroxyl radicals which do not show the experimental markers of tunneling is also examined.

$$R_2NO^{\bullet} + R_2NOH \rightarrow R_2NOH + R_2NO^{\bullet} \quad (1)$$

Hydrogen atom transfer (HAT) has been studied for over a century[6] and is the simplest chemical reaction that involves the transfer of two particles, a proton and an electron. It can therefore be considered to be a type of 'proton-coupled electron transfer' (PCET).[7,8] HAT is important in combustion and selective oxidation of alkanes, in the formation and reactivity of protein-based radicals and reactive oxygen species (ROS), and many other processes.[9] For example, HAT from the double allylic C–H bond in linoleic acid to the iron(III)-hydroxide active site in lipoxygenases has received particular attention because its H/D KIE of up to ~80 indicates the importance of tunneling.[5a,10] HAT involving of nitroxyl radicals and hydroxylamines is important in much of the chemistry of nitroxyl radicals,[11] such as their role as catalysts and co-catalysts in oxidation of organic substrates.[12-13 14 15] *N*-hydroxyphthalimide (NHPI) has been widely explored as a co-catalyst in Co/Mn-catalyzed autoxidations of alkylaromatics, with the active species being the corresponding phthalimide *N*-oxyl radical (PINO$^{\bullet}$).[16] HAT reactions from benzylic C-H bonds to PINO$^{\bullet}$ in acetic acid have large deuterium KIEs (17−28 at 298 K)[17] and the pseudo self-exchange reaction between PINO$^{\bullet}$ and 4-Me-NHPI in acetic acid has k_H/k_D = 11.0 (k_H = 677 ± 24 M^{-1} s^{-1}).[18] Reactions of nitroxyl radicals with arylhydroxylamines, however, exhibit much smaller KIEs, with k_H/k_D = 1.5−1.9 at ambient temperatures (see Table 2 below).[13,14]

We have focused on HAT self-exchange reactions, such as the nitroxyl/hydroxylamine reactions examined here (eq 1), both because of their relative simplicity and because of our finding that the Marcus cross relation usually predicts HAT rate constants within an order of magnitude or two.[19 20-21] This treatment is a new approach to understanding HAT rate constants[22] and has been found to hold for both organic reactions and examples involving transition metal complexes. For instance, the cross relation predicts and explains the inverse temperature dependence of the rate of HAT from $[Fe^{II}(H_2bip)_3]^{2+}$ to the stable nitroxyl radical TEMPO$^{\bullet}$ (2,2,6,6-tetramethylpiperidine-1-oxyl radical).[20] Of the various HAT reactions involving TEMPO$^{\bullet}$ / TEMPO-H and transition metal complexes that we have examined,[19, 20,23,24] the Marcus approach appears to be least accurate for $Ru^{II}(acac)_2(py\text{-}imH)$ + TEMPO$^{\bullet}$ → TEMPO-H and $Ru^{III}(acac)_2(py\text{-}im)$, which has a large KIE.[24b] These results prompted our examination of nitroxyl/hydroxylamine self-exchange reactions; the kinetics of 4-oxo-TEMPO$^{\bullet}$ plus TEMPO-H were briefly mentioned in a preliminary communication about the $[Fe^{II}(H_2bip)_3]^{2+}$ reaction.[20]

Results

I. Equilibrium Constants

The reaction of 4-oxo-TEMPO$^{\bullet}$ and TEMPO-H in CD_3CN forms an equilibrium mixture with 4-oxo-TEMPO-H and TEMPO$^{\bullet}$ (eq 2), with all four species observed by ^{1}H NMR spectroscopy. All of the resonances have been assigned for the

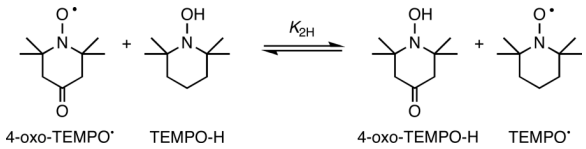

(2)

paramagnetic and diamagnetic species, even though 4-oxo-TEMPO-H has not been isolated. Equilibrium is rapidly established (see below) and integration of each species using Lorentzian line fitting gave $K_{2H,CD3CN} = 4.5 \pm 1.8$ at 298 K.[25] In CD_2Cl_2, $K_{2H,CD2Cl2} = 7.6 \pm 2.4$ was measured similarly. As expected, the equilibrium constants for deuterium atom transfer in CD_3CN and CD_2Cl_2 (K_{2D}), measured using TEMPO-D, are within experimental error of being the same as the K_{2H} values (Table 1). The equilibrium constants are the averages of three independent measurements. All errors reported herein are ± 2σ.

HAT equilibria are also rapidly established between 4-oxo-TEMPO• and 4-MeOTEMPO-H (eq 3) and between ^{t}Bu$_2$NO• and TEMPO-H (eq 4; Table 1). The measured uphill free energy for reaction 4, $\Delta G^o_{4H,CD3CN} = 1.3 \pm 0.1$ kcal mol^{-1}, is very close to the 1.5 kcal mol^{-1} difference in O–H bond dissociation enthalpies (ΔBDE) of TEMPO-H (69.7 kcal mol^{-1}) and ^{t}Bu$_2$NOH (68.2 kcal mol^{-1}) reported by Bordwell in DMSO.[26]

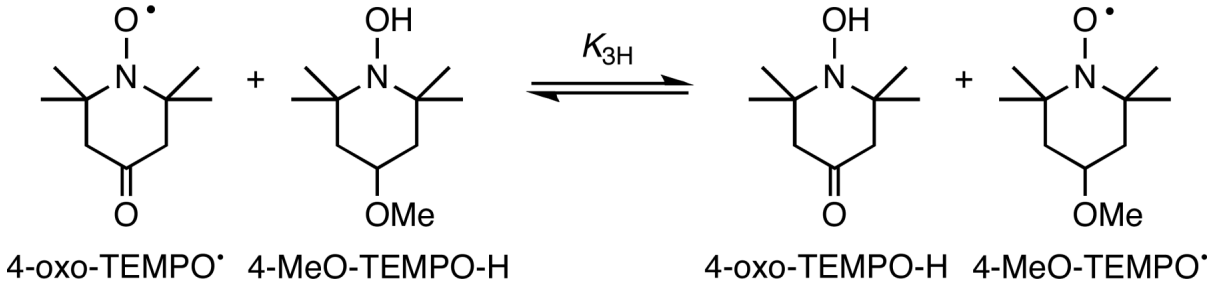

(3)

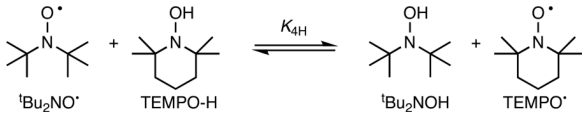

(4)

The equilibrium constants for H and D transfer were determined at temperatures from 278−318 K for reactions 2−4 in CD_3CN (Figure 1) and for reactions 2 and 4 in CD_2Cl_2 (Figure S1; Table 1). Van't Hoff analysis yields small ground state reaction enthalpies and entropies, $|\Delta H^o| \leq 3.1$ kcal mol^{-1} and $|\Delta S^o| \leq 5.8$ cal mol^{-1} K^{-1}. These values support the hypothesis that reactions 2−4 can be regarded as pseudo self-exchange reactions. Small values of ΔS^o are also typical of organic HAT reactions, even for those that are not self-exchange reactions.[23]

II. Kinetic Measurements

Attempts to directly measure the rate of HAT self-exchange between TEMPO• and TEMPO-H by ^{1}H NMR line broadening were unsuccessful.[27] Therefore, we have studied the pseudo self-exchange reactions in eqs 2-4 using stopped-flow optical measurements. The reaction between 4-oxo-TEMPO• and TEMPO-H (eq 2), for instance, is readily monitored by UV-vis

spectroscopy because the spectrum of 4-oxo-TEMPO• in MeCN (λ_{max} = 440 nm, ε = 5.5 M^{-1} cm^{-1}) is different from that of TEMPO• (λ_{max} = 460 nm, ε = 10.3 M^{-1} cm^{-1}), particularly in ε.

The reaction kinetics have been measured by UV-vis stopped flow techniques under pseudo first order conditions, with an excess of TEMPO-H (59−292 mM, ≥10 equiv) over 4-oxo-TEMPO• (5.9−12 mM) in MeCN (Figure 2a). Under these conditions the reaction proceeds essentially to completion ($K_{2H,MeCN}$ = 4.5). The optical data were fitted across the whole spectral region (350−550 nm) using SPECFIT global analysis software.[28] The data fit well to a simple first-order A → B model (Figure 2b), and the pseudo first-order rate constants k_{obs} are independent of the initial concentration of 4-oxo-TEMPO•. Plotting k_{obs} versus [TEMPO-H] yields a straight line (Figure 3), indicating a first order dependence on [TEMPO-H] and a bimolecular rate constant for the forward reaction in eq 2 of $k_{2H,MeCN}$ = 10 ± 1 M^{-1} s^{-1} at 298 K. Reactions with less TEMPO-H, under second order approach-to-equilibrium conditions A + B ⇄ C + D, gave the same value of $k_{2H,MeCN}$ within error.

To investigate the role of solvent, the same kinetic experiments were performed in CH_2Cl_2 and CCl_4 solutions. Analysis as above gave $k_{2H,CH2Cl2}$ = 48 ± 4 M^{-1} s^{-1} (Figure 3) and $k_{2H,CCl4}$ = 300 ± 30 M^{-1} s^{-1} at 298 K. These rate constants are, respectively, 4.8 and 30 times larger than in MeCN.

The KIE for reaction 2 was examined using TEMPO-D prepared by TEMPO• reduction with $Na_2S_2O_4$ in acetone-d_6/D_2O. This TEMPO-D, which was 98 ± 1% D by ^1H NMR integration, reacts with 4-oxo-TEMPO• in MeCN with $k_{2D,MeCN}$ = 0.44 ± 0.05 M^{-1} s^{-1} (Figure 3). This rate constant is 23 ± 3 times slower than that for the same reaction of TEMPO-H at 298 K. Within experimental error, essentially the same apparent isotope effects are found in CH_2Cl_2, 23 ± 4, and in CCl_4, 18 ± 5. Thus solvent polarity and hydrogen bonding to solvent do not significantly affect the KIEs. The ratio of the rate constants, however, is only a lower limit to the true KIE because the residual 2 ± 1% H in the TEMPO-D contributes significantly to the reactions. If the TEMPO-D was 99% D, the true KIE would be 30, and if it was 97% D, the true KIE would be 72.[29] These are the experimental bounds on the KIE.

The kinetics of 4-oxo-TEMPO• plus excess 4-MeO-TEMPO-H (eq 3) in MeCN were measured and analyzed in a similar fashion, to give k_{3H} = 7.8 ± 0.7 M^{-1} s^{-1} at 298 K (Figure S2). This is about 20% lower than the rate constant for reaction 2 under the same conditions, which is consistent with the equilibrium constant for reaction 3, $K_{3H,MeCN}$ = 2.8 ± 1.2, being a little smaller than $K_{2H,MeCN}$ = 4.5 ± 1.8 for reaction 2.

Similar to the case for reaction 2, the rate constant for reaction of the deuterated hydroxylamine, 4-MeO-TEMPO-D, at 298 K is much slower, k_{3D} = 0.37 ± 0.05 M^{-1} s^{-1} (Figure S2), than that for the reaction of the undeuterated compound. Since the 4-MeO-TEMPO-D is also 98 ± 1% deuterated, the k_{3H}/k_{3D} = 21 ± 3 at 298 K is also a lower limit to the true KIE. Rate constants and k_H/k_D values at 298 K for the forward reactions 2−4 are given in Table 2, along with the rate constants for other nitroxyl plus hydroxylamine reactions.

The reaction of $^tBu_2NO$• and TEMPO-H (eq 4) in MeCN is uphill in free energy ($K_{4H,MeCN}$ = 0.11), so the kinetics were measured by UV-vis stopped flow techniques under second order approach-to-equilibrium conditions. The optical spectra of $^tBu_2NO$• (λ_{max} = 454 nm, ε = 8.9 M^{-1} cm^{-1}) and TEMPO• (λ_{max} = 460 nm, ε = 10.3 M^{-1} cm^{-1}) are similar, so the overall change of the absorbance is small (Figure S3). Under the experimental conditions ([$^tBu_2NO$•] =12−139 mM, [TEMPO-H] = 118−237 mM), spectra of reaction mixtures at short times show absorbances ~10% higher than equimolar solutions of $^tBu_2NO$•, suggesting partial formation of a complex between $^tBu_2NO$• and TEMPO-H. Consistent with this suggestion, adding 2,4,6-

tri-*tert*-butylphenol to solutions of $^{t}Bu_2NO^{\bullet}$ caused similar changes in optical spectra, even though HAT does not occur ($\Delta BDE = +14$ kcal mol^{-1}).[30] These changes in reaction 4 are subtle, however, and are too small to enable determination of a value for the equilibrium constant. There are also subtle differences between the final reaction spectrum and that of TEMPO$^{\bullet}$, suggesting that the products could also be, in part, hydrogen-bonded.

The forward bimolecular rate constant for eq 4 under these conditions, $k_{4H,MeCN}$, is 1.9 ± 0.2 M^{-1} s^{-1} at 298 K, as determined by fitting the data to an opposing second order equilibrium model (A + B ⇄ C + D) with a fixed $K_{4H,MeCN} = 0.11$, using SPECFIT[28] (Figure S3). When TEMPO-D is used, the initial spectra of the reaction mixtures are much closer to those of solutions of pure $^{t}Bu_2NO^{\bullet}$, suggesting that adduct formation is isotopically sensitive, and is less favorable for TEMPO-D than for TEMPO-H. The rate constant for D-atom transfer, $k_{4D,MeCN} = 0.12 \pm 0.02$ M^{-1} s^{-1} indicates $k_{4H,MeCN}/k_{4D,MeCN} = 16 \pm 3$ at 298 K. Reaction 4 behaves similarly in CH_2Cl_2 solvent, showing a similar isotope effect: $k_{4H,CH2Cl2}/k_{4D,CH2Cl2} = 13 \pm 2$.

Rate constants for reactions 2−4 have been measured as a function of temperature over 35−40 K temperature ranges. Selected Eyring plots are shown in Figure 4, and all Eyring and Arrhenius activation parameters are listed in Table 3. Table 4 shows the difference between the H versus D activation energies ($E_{aD} - E_{aH}$) and pre-exponential factors, $\log(A_H/A_D)$.

III. Computational Studies

In order to investigate the role of tunneling in self-exchange reactions between nitroxyl radicals and hydroxylamines, we performed multi-dimensional tunneling calculations, using GAUSSRATE[31] as the interface between Gaussian 03[32] and POLYRATE.[33] Our computations were carried out using both the MPW1K[34] and the more recently developed MO5−2X[35] and MO6[36] functionals. The 6−31+G(d,p) basis set[37] was employed for all of these calculations. Tunneling rates were computed, using the small-curvature tunneling (SCT) approximation.[38]

Because of the computational demands of the SCT tunneling calculations, calculations on the $^{t}Bu_2NO^{\bullet}$ + $^{t}Bu_2NOH$ and TEMPO$^{\bullet}$ + TEMPO-H systems were too big to be practical. Therefore, we began by performing calculations on $(CH_3)_2NO^{\bullet}$ + $(CH_3)_2NOH$. The calculated rate constants, activation parameters, and H/D kinetic isotope effects for this reaction are given in Table 5.

The transition structure (TS) for $(CH_3)_2NO^{\bullet}$ + $(CH3)_2NOH$, shown in Figure 5a, has C_{2h} symmetry. The SCT calculations start at this TS and descend down a minimum energy path toward the reactants/products. Unfortunately, starting from the TS and moving along this reaction coordinate, the C_s plane of symmetry was maintained throughout the reaction. Consequently, the SCT calculations did not lead to the hydrogen-bonded reactant complex $(CH_3)_2NOH...^{\bullet}ON(CH_3)_2$, which has C_1 symmetry (Figure 5b). Instead, the calculations led to the C_s TS that connects the two enantiomeric geometries of the reactant complex. Destroying the C_s plane in the C_{2h} TS by substituting two CD_3 for two CH_3 groups failed to coax the hydrogen-bonded complex to depart from the ridge on the potential energy surface that connects the two enantiomers.

However, we were able to follow the reaction path back from the TS to the reactants for the self-exchange reaction between the monomethylnitroxyl radical and the monomethylhydroxylamine. The calculated values of k_H, E_a, A, and k_H/k_D for this reaction, $(CH_3)HNO^{\bullet}$ + $HONH(CH_3)$, are also given in Table 5. The two reactions are close enough to lead us to believe that the computational results for the dimethyl reaction are reliable, despite our being unable to follow the reaction path all the way back to the reactant complex in this case. Most of the tunneling seems to originate from regions along the reaction path that are

closer to the TS, where the reaction barrier is narrow, than from regions close to the reactants, where the barrier is much wider and the deviation from C_s symmetry is significant.

The formation of the $(CH_3)_2NOH...^{\bullet}ON(CH_3)_2$ reactant complex (Figure 5B) from the separated reactants is enthalpically favorable: $\Delta H = -4.6$ kcal mol^{-1} [calculated with MPW1K/6−31+ G(d,p)]. However, the entropy of complex formation [$\Delta S = -26.7$ cal K^{-1} mol^{-1}] is so unfavorable that the calculated value of the gas phase equilibrium constant [$K = 1.4 \times 10^{-4}$ M^{-1}] at 298 K is small. Since at 298 K the reactants are lower in free energy than the reactant complex, the computed rate constants, *A* factors, and activation energies reported in Table 5 are for reactions starting from the separated reactants.

We used all three functionals -- MPW1K, MO5−2X, and MO6 -- to calculate the barrier height for the hydrogen self-exchange reaction, $(CH_3)_2NO^{\bullet} + (CH_3)_2NOH$, starting from the C_1 reactant complex. All three functionals gave enthalpies of activation for passage over the reaction barrier that were the same to within 1.0 kcal mol^{-1}. Therefore, we elected to do the tunneling calculations with just one of them, MPW1K.

The MPW1K rate constants at 298 K for the hydrogen and deuterium self-exchange reactions were computed by canonical variational transition state theory (CVT) for passage over the barrier and by small curvature tunneling (SCT) calculations for passage through the barrier. The results are contained in Table 5. The Arrhenius activation parameters, obtained from the temperature dependences of the calculated rate constants around 298 K, are also given in Table 5.

The k_H values in Table 5 show that the SCT rate constant for hydrogen tunneling through the barrier is computed to be larger than the CVT rate constant for passage over it by a factor of about 10^5. Tunneling reduces E_a by 8.7 kcal mol^{-1} for hydrogen, with a decrease in log *A* of only 1.4. The large reduction in E_a and the small decrease in log *A* shows that our SCT calculations predict that tunneling is very efficient in $(CH_3)_2NO^{\bullet} + (CH_{3)2}NOH$. The width of the barrier to this reaction is computed to be only 0.42 Å, which is presumably why tunneling is computed to be so effective at increasing the reaction rate.

Table 5 also contains the results of our calculations for deuterium self-exchange in $(CH_3)_2NO^{\bullet} + (CH_3)_2NOD$. Comparison of the CVT and SCT rate constants for D shows that tunneling is also predicted to dominate the reaction involving deuterium. However, a very large H/D KIE of $k_H/k_D = 196$ is predicted for tunneling. Of this ratio, a factor of 7.4 is due to H tunneling with a 1.2 kcal mol^{-1} lower E_a, than D. An even larger factor is due to log A_H being about 1.4 larger than log A_D. Even though H is calculated to tunnel through the barrier at an average energy of about 1.2 kcal mol^{-1} lower than D, H is calculated to tunnel with a higher probability than D by a factor of 26.5.[39]

Our SCT value of H/D KIE of 196 for $(CH_3)_2NO^{\bullet} + (CH3)_2NOH/D$ is about a factor of 5 larger than the experimental values for reaction of TEMPO-H with a variety of nitroxide radicals (Table 2). However, as already noted, the true H/D KIEs are substantially larger than the values given in Table 2, because of the incomplete D enrichment. For TEMPO-H/D + 4-oxo-TEMPO$^{\bullet}$, the measured k_H/k_D of 23 at 98 ± 1% D corresponds to a true KIE of about 40 (the 98 ± 1% range gives values of 30−70).

The calculated bimolecular SCT rate constant of $k = 48.5$ M^{-1} s^{-1} is in excellent agreement with the rate constants in Table 2 for the TEMPO-H reactions. The closest experimental analogy to this gas phase rate constant is the *k* of 300 M^{-1} s^{-1} for 4-oxo-TEMPO$^{\bullet}$ + TEMPO-H in CCl_4, which has $\Delta G^o \cong -1$ kcal mol^{-1}. In contrast, the CVT rate constant of $k = 5.65 \times 10^{-4}$ M^{-1}s^{-1} for $(CH3)_2NO^{\bullet} + (CH3)_2NOH$ underestimates the experimental rate constants (Table 2) by a factor of $10^4 - 10^6$. Thus, our calculations on both the rate of and H/D KIE for

this model reaction strongly support the conclusion that the dialkylnitroxyl radical reactions in Table 2 all occur by tunneling through the reaction barrier, rather than by passage over it.

Although we were unable to perform SCT calculations on larger systems, we did carry out CVT calculations on the $^{t}Bu_2NO(^{\bullet}/H)$, TEMPO($^{\bullet}$/H) and $Ph_2NO(^{\bullet}/H)$ self-exchange reactions. For each one, the TS was located and confirmed to have one imaginary frequency by a vibrational analysis. Key features of the geometries of the nitroxide reactants and the self-exchange TSs are given in Figure 6, along with the calculated E_a values from CVT for each reaction.

As shown in Figure 6, the geometries of the TSs for all three reactions are very similar. In each TS the O-H bonds approximately bisect the C-N-C angles, strongly suggesting that the electron and the proton are transferred together between the same AO on each oxygen. This inference is confirmed by inspection of the SOMOs for the three TSs, which are shown in Figure 7. Thus, all three reactions proceed by a mechanism in which a hydrogen atom is transferred between a pair of oxygen AOs, rather than by a mechanism in which a proton is transferred between one pair of oxygen AOs and an electron is transferred between a different pair of oxygen AOs (which in some contexts has been called proton-coupled electron transfer, PCET).[40]

The CVT activation energies for the dialkylnitroxyl reactions, E_a = 15.7 and 14.5 kcal mol^{-1} for $^{t}Bu_2NO^{\bullet}$ + $^{t}Bu_2NOH$ and TEMPO$^{\bullet}$ + TEMPO-H, respectively, are much larger than the corresponding energy for $Ph_2NO^{\bullet}$ + Ph_2NOH, 5.6 kcal mol^{-1}. This is in pleasing agreement with the experimental finding that the rate constant for $Ph_2NO^{\bullet}$ + Ph_2NOH[13] is at least five orders of magnitude faster than those for $^{t}Bu_2NO^{\bullet}$ + $^{t}Bu_2NOH$[13] and TEMPO$^{\bullet}$ + TEMPO-H. Comparisons of the geometries and spin densities of the nitroxide reactants and TSs in Figure 6 indicates that the phenyl groups lower the barrier to reaction by providing greater delocalization of the unpaired electron in the TS for $Ph_2NO^{\bullet}$ + Ph_2NOH reaction than in the Ph_2NO reactant.

In the nitroxyl radicals, the unpaired spin density of 0.88 in the N-O group of $Ph_2NO^{\bullet}$ is about 0.1 smaller than the unpaired spin densities of 0.98 and 1.00 in the NO groups of TEMPO$^{\bullet}$ and $^{t}Bu_2NO^{\bullet}$, respectively. The C-N bond lengths in $Ph_2NO^{\bullet}$ are calculated to be 0.07 and 0.08 Å shorter than those in TEMPO and $^{t}Bu_2NO^{\bullet}$, respectively. This is a larger difference than the ~0.04 Å difference in covalent radii between sp^2 and sp^3 carbon atoms. These results indicate that the phenyl groups in $Ph_2NO^{\bullet}$ delocalize the unpaired electron in the two-center, three-electron N-O π bond.

On going from the reactants to the TS, the four C-N bond lengths in $Ph_2NO^{\bullet}$ shorten by an average of 0.02 Å; whereas the C-N bond lengths in TEMPO$^{\bullet}$ and $^{t}Bu_2NO^{\bullet}$ shorten by less than 0.01 Å. In addition, the spin densities in the NO groups of the $Ph_2NO^{\bullet}$ + Ph_2NOH TS are 0.08 smaller than the spin density in the NO group of $Ph_2NO^{\bullet}$; whereas, the corresponding decrease in the spin densities in the NO groups is only about 0.03 in both TEMPO$^{\bullet}$ + TEMPO-H and $^{t}Bu_2NO^{\bullet}$ + $^{t}Bu_2NOH$. The larger decreases in the C-N bond lengths and in the NO spin densities between the $Ph_2NO^{\bullet}$ reactants and the TS for $Ph_2NO^{\bullet}$ + Ph_2NOH are both consistent with the TS for this reaction being stabilized by electron delocalization into the phenyl groups. We believe that this is the reason why the hydrogen self-exchange reaction of this diarylnitroxyl radical is many orders of magnitude faster than those of the dialkylnitroxyl radicals in Table 2.

Discussion

Nitroxyl radical plus hydroxylamine reactions have been studied experimentally and computationally. The experimental reactions (eqs 2-4) are close to isoergic in both MeCN and

CH_2Cl_2, with $|\Delta G^o| \leq 1.4$ kcal mol^{-1} (Table 2), and involve reagents that are sterically quite similar. Thus these reactions are good approximations of self-exchange reactions. Self-exchange reactions are inherently simpler to analyze because of their symmetry, which requires that the transition structure, or more generally the seam on the potential energy surface, be symmetrically placed between the reactant and product.

Thermochemical data show that the reactions must occur by concerted rather than stepwise transfer of the proton and electron. For self-exchange reactions, the potential stepwise mechanisms with initial electron or proton transfer are the microscopic reverse of each other.[41] For the TEMPO$^{\bullet}$ + TEMPO-H self-exchange reaction, both stepwise pathways proceed through a TEMPO$^-$ + TEMPO-H$^{\bullet+}$ intermediate state. Based on the known $E_{1/2}$ and pK_a values, this state is about 60 kcal mol^{-1} higher than TEMPO$^{\bullet}$ + TEMPO-H (2.6 V or 44 pK_a units).[42] For the pseudo self-exchange reactions in eqs 2-4, the data are not available to make a full analysis, but the $E_{1/2}$ and pK_a values are not very different for the various compounds,[26] so these reactions will also have potential intermediate states lying *ca*. 60 kcal mol^{-1} uphill. This is dramatically higher than the Eyring barriers $\Delta G^{\ddagger} < 20$ kcal mol^{-1} found for reactions 2−4. Thus the stepwise pathways are not possible and the reaction must occur by concerted H^+/e^- transfer.

I. Solvent Effects

The experimental rate constants are faster in less polar and less hydrogen-bonding solvents (Table 2). For 4-oxo-TEMPO$^{\bullet}$ + TEMPO-H, the rate constants are 10, 48, and 300 M^{-1} s^{-1} in MeCN, CH_2Cl_2, and CCl_4, respectively. Litwinienko, Ingold, et al. have shown that for HAT reactions of phenols, solvent effects on the rate constants are predominantly due to the formation of a hydrogen bond between the H-atom donor and the solvent.[43] Only the fraction of the phenol that is not hydrogen bonded is reactive, and the reactivity of the non-hydrogen bonded phenol is not significantly affected by solvent. Qualitatively, this explains why the TEMPO-H reactions are slower in MeCN, a good hydrogen bond acceptor, than in chlorinated solvents. The formation of TEMPO-H•••NCMe hydrogen bonds is indicated by the TEMPO-H O–H stretching frequency in CD_3CN (3495 cm^{-1}), being ~100 cm^{-1} lower than ν(TEMPO-H) in CD_2Cl_2 (3583 cm^{-1}) and CCl_4 (3597 cm^{-1}). A recent crystal structure of TEMPO-H shows hydrogen bonds between TEMPO-H molecules with O...O distances of 2.83 and 2.88 Å.[23]

Quantitatively, the Litwinienko and Ingold model predicts that the solvent effect will be independent of the H-atom acceptor.[44,45] However, the experimental ratios of rate constants in CH_2Cl_2 vs. MeCN are 4.8 ± 0.6 for 4-oxo-TEMPO$^{\bullet}$ + TEMPO-H and 2.4 ± 0.3 for ^{t}Bu$_2$NO$^{\bullet}$ + TEMPO-H.[44] The 4-oxo-TEMPO$^{\bullet}$ + TEMPO-H reaction (eq 2) appears to be affected by solvent polarity as well as hydrogen bonding, as it is 6 times faster in CCl_4 than in CH_2Cl_2 (Table 2). A more dramatic effect has been reported for the ^{t}BuArNO$^{\bullet}$/^{t}BuArNOH self-exchange reaction (Ar = 2,6-dimethoxyphenyl), which is more than a hundred times faster in CCl_4 than in $CHCl_3$ and CH_2Cl_2: 2×10^3 versus < 20 M^{-1} s^{-}.[13] A reviewer has suggested that these anomalous kinetic solvent effects may be due to changes in the nitroxyl radical spin density with solvent,[46] which are known to affect their rate constant for reaction with alkyl radicals.[47]

II. Kinetic Isotope Effects and Evidence for Tunneling

Hydrogen tunneling is suggested by the large k_H/k_D values of 23 ± 3, 21 ± 3, and 16 ± 3 at 298 K for reactions 2−4 in MeCN. A one-dimensional semi-classical transition state theory model, taking $\Delta G^{\ddagger}_D - \Delta G^{\ddagger}_H$ to be at most the difference in zero-point energies, predicts a maximum k_H/k_D of 9 at 298 K using the measured OH and OD stretches.[3,4,48] A more complete semi-classical model including bending modes gives a maximum KIE of about 13 for cleavage of

an O–H bond.[3] The computed CVT H/D KIEs at 298 K, without tunneling, are 6.5, 4.9, 4.9, and 4.7 for the self-exchange reactions involving $Me_2NO^{\bullet}$, $^{t}Bu_2NO^{\bullet}$, TEMPO$^{\bullet}$, and $Ph_2NO^{\bullet}$. These computed H/D KIEs are all significantly lower than the measured values for reactions 2−4, but they are *ca*. three times larger than the KIEs in Table 2 for reactions involving monoarylhydroxylamines, including the ^{t}Bu(Ar)NO$^{\bullet}$ + ^{t}Bu(Ar)NOH self-exchange [Ar = 2,6-$(MeO)_2C_6H_3$].

The experimental activation energies also provide evidence for tunneling. According to Bell, [3] tunneling is indicated when $E_{aD} - E_{aH}$ is larger than the difference in zero-point energies, 1.3 kcal mol^{-1} in this case,[48] and/or when there are significant differences in the pre-exponential terms, $A_H/A_D < 0.7$ or $A_H/A_D > 1.4$, or $|\log(A_H/A_D)| > 0.15$. All of the reactions studied here have $\log(A_H/A_D)$ larger than this semi-classical limit, except perhaps for reaction 2 in MeCN which has $\log(A_H/A_D) = 0.5 \pm 0.7$ (Table 4). For reactions 2 and 3, the positive values of $\log(A_H/A_D)$, the low values of both A_H and A_D (<10^5 M^{-1} s^{-1}), and low E_a (<6 kcal mol^{-1}) values all suggest that there is significant tunneling in the reactions of both the H and D isotopomers.[5]

The small-curvature tunneling calculations on $(CH_3)_2NO^{\bullet}$ + $(CH_3)_2NOH$ also show that tunneling is the dominant pathway in this model reaction for a self-exchange involving a dialkylnitroxyl radical reacting with a dialkylhydroxylamine. Tunneling through the barrier is computed to be about 10^5 times faster than passage over the barrier for H, and more than 10^3 times faster, even for D. The experimental KIEs vary little with solvent – between MeCN, CH_2Cl_2, and CCl_4 for reaction 2, and between MeCN and CH_2Cl_2 for reaction 4 – indicating that the solvent plays little role in the tunneling process.[49]

The $^{t}Bu_2NO^{\bullet}$ + TEMPO-H reaction (eq 4) is found to have very unusual activation parameters. These data derive from quite small changes in absorbance (see above), but they are based on three separate measurements of rate constants at each temperature, with consistent multiple stopped-flow runs in each measurement. The resulting A_H is a thousand times larger than A_D both in MeCN and CH_2Cl_2, and E_{aD} is substantially smaller than E_{aH}: $E_{aD} - E_{aH} = -2.5 \pm 0.4$ in MeCN and -3.1 ± 0.4 kcal mol^{-1} in CH_2Cl_2. That $E_{aD} < E_{aH}$ is indicated by the increase in k_{4H}/k_{4D} values with temperature, in MeCN from 11 ± 1 at 278 K to 17 ± 2 at 308 K and 21 ± 6 at 318 K. These values are surprising both because they are so different than those for the very similar reactions 2 and 3,[50] and because $E_{aD} < E_{aH}$ is opposite to the predictions of both semi-classical and tunneling models.[3,5] While similar unusual activation parameters have been reported for two other HAT/PCET reactions,[51] we are not sure of the origin in this case. It is interesting that the formation of the hydrogen-bonded precursor complex in this reaction, TEMPO-H/D...$^{\bullet}$ON$^{t}Bu_2$, also appears to be isotopically sensitive (see above).[17,52]

In light of the importance of tunneling for the TEMPO$^{\bullet}$/TEMPO-H self-exchange reaction, the success of the Marcus cross relation for reactions involving TEMPO$^{\bullet}$ is perhaps surprising. The cross relation is a semiclassical treatment that does not include hydrogen tunneling. Still, the cross relation is essentially interpretative, and will still hold if the self-exchange and cross reactions are accelerated a comparable amount by tunneling.

III. Comparison with related reactions

The rate constants for nitroxyl + hydroxylamine self-exchange and pseudo self-exchange reactions show a remarkable range, from 2 to >10^7 M^{-1} s^{-1} (Table 2). Other XO$^{\bullet}$ + XOH reactions show similar variation: $^{t}Bu_2C{=}NO^{\bullet}$ + $^{t}Bu_2C{=}NOH$ in benzene, 1.3 M^{-1} s^{-1};[53] 2,4,6-$^{t}Bu_3C_6H_2O^{\bullet}$ + 2,4,6-$^{t}Bu_3C_6D_2OH$ in CCl_4, 220 M^{-1} s^{-};[13b] ^{t}BuOO$^{\bullet}$ + ^{s}BuOOH in isopentane, 490 M^{-1} s^{-1};[54] ^{t}BuO$^{\bullet}$ + $^{t}Bu_3COH$ in ^{t}BuOO^{t}Bu, ~3 × 10^4 M^{-1} s^{-1};[55] and PhO$^{\bullet}$ + 2-naphthol ($\Delta G^{o} \approx -2$ kcal mol^{-1}) in MeCN, 4.5 × 10^6 M^{-1} s^{-1}.[52,56] The most striking comparison is from the measurements of R_2NOH + $R_2NO^{\bullet}$ self-exchange reactions by Kreilick

and Weissman in CCl_4: 320 M^{-1} s^{-1} for R = ^{t}Bu vs. >10^7 M^{-1} s^{-1} for R = Ph.[13] The dichotomy between the dialkyl- and arylhydroxylamine reactions is also evident in the HAT kinetic isotope effects. The more rapid arylhydroxylamine reactions have $k_H/k_D < 2$, while the slower dialkylnitroxyl reactions have $k_H/k_D > 10$ (Table 2).

Reactions of the acylnitroxyl PINO$^\bullet$ display yet another pattern of reactivity.[17,18] The pseudo self-exchange reaction of PINO$^\bullet$ with the hydroxyphthalate Me-NHPI has values of E_a (10 kcal mol^{-1}) and A_H ($10^{10.4}$ M^{-1} s^{-1}) that are significantly larger than those of the TEMPO$^\bullet$/4-oxo-TEMPO$^\bullet$/4-MeO-TEMPO$^\bullet$ reactions (eqs 2 and 3): $E_a \leq 6$ kcal mol^{-1} and $A_H \leq 10^5$ M^{-1} s^{-1} (Table 3). The reactions of PINO$^\bullet$ with *p*-xylene and toluene appear to involve tunneling, but in contrast to reactions 2–4, they show large values of $E_{aD} - E_{aH}$ and negative values of log (A_H/A_D) (3.0 ± 0.3 kcal mol^{-1}, −0.8 ± 0.3 for *p*-xylene), suggesting that tunneling is more pronounced for H than for D.[17,18] The related HAT reaction of $(CF_3)_2NO^\bullet$ with toluene, with $k_H/k_D = 13$ and $\log(A_H/A_D) \approx 0$ ($A_H \approx A_D \approx 10_4$), was not suggested to involve significant tunneling.[57]

The diversity of behavior is remarkable for such similar reactions. All of the nitroxyl/hydroxylamine reactions discussed here are close to isoergic ($|\Delta G^o| \leq 2$ kcal mol^{-1}, Table 2) so the driving forces are not the cause of these differences. The differences between the dialkyl- and the arylhydroxylamine reactions could conceivably be largely due to a steric effect. The bulkier tertiary alkyl groups might make assembly of the precursor complex more difficult and could keep the oxygen atoms farther apart. Such a difference in TS geometries would lead to higher barriers and longer H-transfer distances, enhancing the importance of tunneling in the dialkylnitroxyl reactions. However, the results of our calculations show that there is very little difference between the geometries of the TSs for the dialkyl- and diarylnitroxyl self-exchange reactions. Instead, our calculations find that the much faster $Ph_2NO^\bullet$ + Ph_2NOH self-exchange reaction is due to the greater electronic delocalization provided by the phenyl groups in the transition structure. The CVT barrier for $Ph_2NO(^\bullet/H)$ self-exchange reaction, 5.6 kcal mol^{-1}, is 9–10 kcal mol^{-1} lower than the CVT barriers for the $^tBu_2NO(^\bullet/H)$ and TEMPO(H) self-exchange reactions (15.7, 14.5 kcal mol^{-1}, respectively).

Because the reaction barriers for the arylhydroxylamines are lower than those for the dialkylhydroxylamines, the former reactions can proceed by passage over, or close to the top of the barriers, without the need for substantial tunneling. In contrast, the higher reaction barriers on the potential energy surfaces for the dialkylhydroxylamine reactions lead to both H and D preferentially tunneling through the barriers. Tunneling produces the low E_a and *A* values and the high H/D KIEs that we have both measured and calculated for the dialkylnitroxyl radical + dialkylhydroxylamine reactions.

While many discussions of tunneling emphasize the distance over which the H or D transfers must occur, in this case the O-H bond distances in the reactant complexes and transition structures are calculated to be quite similar for the reactions of dialkylhydroxylamines vs. those of arylhydroxylamines. The results of our calculations suggest that the former reactions show the experimental indications of tunneling while the latter do not because of the different barrier heights for degenerate HAT in these two types of hydroxylamines. These studies thus appear to be an experimental example of the well-known theoretical result that barrier height is as key a factor as barrier width in determining the probability of tunneling in a chemical reaction.[3]

Conclusions

Hydrogen atom transfer from dialkylhydroxylamines to dialkylnitroxyl radicals predominantly involves hydrogen tunneling. This has been shown through a combination of experimental and computational studies. Experimentally, the kinetics of three pseudo-self exchange reactions

have been examined. For the reactions of 4-oxo-TEMPO$^{\bullet}$ with TEMPO-H (eq 2) and 4-MeO-TEMPO-H (eq 3), the activation parameters and H/D kinetic isotope effects (Tables 2-4) suggest that tunneling is important in both H and D transfers. The measured ratios of k_H/k_D = 21−23 ± 4 correspond to intrinsic KIEs of ca. 40 at 298 K, given the 98 ± 1% deuterium enrichment of the hydroxylamines. Computational studies of the $(CH_3)_2NO^{\bullet}$ + $(CH_3)_2NOH$ model reaction, using the small-curvature tunneling (SCT) approximation, also find substantial tunneling by both H and D. The reaction of $^tBu_2NO^{\bullet}$ with TEMPO-H (eq 4) has very unusual activation parameters, with $E_a(D) < E_a(H)$ and $\log(A_H/A_D) \approx 3$.

The properties of these pseudo self-exchange reactions of dialkylhydroxylamines contrast with related reactions of *aryl*hydroxylamines. Aryl-substituted hydroxylamines generally react with higher rate constants and very small KIEs (< 2). Calculations indicate that the $Ph_2NO^{\bullet}$ + Ph_2NOH self-exchange has a 9−10 kcal mol^{-1} lower barrier than the $^tBu_2NO^{\bullet}$ + $^tBu_2NOH$ and TEMPO + TEMPO-H self-exchange reactions, due to greater electron delocalization in the $[Ph_2NO..{}_{H}..{}_{ONPh2}]^{\bullet}$ transition structure. The picture that emerges from these studies is that the self-exchange reactions of the dialkylhydroxylamines involve tunneling of both H and D, while the related reactions of arylhydroxylamines proceed over or close to the top of the reaction barriers. This dichotomy is due to the higher barriers for the dialkylhydroxylamine reactions, rather than to differences in the geometries of the reactant complexes or transition structures between the two types of hydroxylamines.

Experimental

Physical Techniques and Instrumentation

^1H (500 MHz) and $^{13}C\{^1H\}$ (126 MHz) NMR were recorded on Bruker Avance spectrometers, referenced to a residual solvent peak, and reported as: δ (multiplicity, assignment, number of protons). The error for NMR integration is estimated to be ±10%. Lorentzian line fitting for accurate integration was done using NUTS.[25] Electrospray ionization mass spectra (ESI/MS) were obtained on a Bruker Esquire-LC ion trap mass spectrometer and reported as *m/z*, with samples infused as MeCN solutions. UV-vis spectra were acquired with a Hewlett-Packard 8453 diode array spectrophotometer, and reported as λ_{max}/nm (ε/M^{-1} cm^{-1}). IR spectra were obtained as CD_3CN, CD_2Cl_2, or CCl_4 solutions in a NaCl solution cell, using a Bruker Vector 33 or Perkin Elmer 1720 FT-IR spectrometer, and reported in cm^{-1}. UV-vis stopped-flow measurements were obtained on an OLIS RSM-1000 stopped-flow spectrophotometer. Elemental analyses were performed by Atlantic Microlab (Norcross, GA). All reactions were performed in the absence of air using standard glove box/vacuum line techniques.

Materials

All reagent grade solvents were purchased from Fisher Scientific, EMD Chemicals, or Honeywell Burdick & Jackson (for anhydrous MeCN). Deuterated solvents were obtained from Cambridge Isotope Laboratories. CD_3CN was dried over CaH_2, vacuum transferred to P_2O_5, and over to CaH_2, then to a dry glass flask. CD_2Cl_2 was dried over CaH_2, and vacuum transferred to a dry glass flask. TEMPO$^{\bullet}$, 4-oxo-TEMPO$^{\bullet}$, 4-MeO-TEMPO$^{\bullet}$, and $^tBu_2NO^{\bullet}$ were purchased from Aldrich, and were sublimed onto a cold-finger apparatus before use. UV-vis (MeCN): TEMPO$^{\bullet}$, 460 (10.3); 4-oxo-TEMPO$^{\bullet}$, 440 (5.5); 4-MeO-TEMPO$^{\bullet}$, 460 (10.4); $^tBu_2NO^{\bullet}$, 454 (8.9). UV-vis (CH_2Cl_2): TEMPO$^{\bullet}$, 460 (11.1); 4-oxo-TEMPO$^{\bullet}$, 446 (6.0); 4-MeO-TEMPO$^{\bullet}$, 462 (11.0); $^tBu_2NO^{\bullet}$, 450 (9.0). UV-vis (CCl_4): TEMPO$^{\bullet}$, 471 (12.2); 4-oxo-TEMPO$^{\bullet}$, 450 (7.1). Anal. Calcd (Found) for TEMPO$^{\bullet}$ ($C_9H_{18}NO$): C, 69.18 (69.14); H, 11.61 (11.65); N, 8.96 (9.09); for 4-oxo-TEMPO$^{\bullet}$ ($C_9H_{16}NO_2$): C, 63.50 (63.61); H, 9.47 (9.51); N, 8.23 (8.19); for 4-MeO-TEMPO$^{\bullet}$ ($C_{10}H_{20}NO_2$): C, 64.48 (64.64); H, 10.82 (10.97); N, 7.52 (7.47); for $^tBu_2NO^{\bullet}$ ($C_8H_{18}NO$): C, 66.62 (66.87); H, 12.58 (12.79); N, 9.71 (9.61).

TEMPO-H was prepared according to literature procedures.[58] ^{1}H NMR (CD_3CN): δ 1.06 (s, CH_3, 12H), 1.45 (s, CH_2, 6H; the C3/C5 and C4 signals are coincident), 5.34 (br s, OH, 1H). ^{1}H NMR (CD_2Cl_2): δ 1.10 (s, CH_3, 12H), 1.46 (s, CH_2, 6H), 4.31 (br s, OH, 1H). ^{13}C{^{1}H} NMR (CD_3CN): δ 17.78 (C4), 26.11 (CH_3), 40.16 (C3), 58.78 (C2). Anal. Calcd (Found) for TEMPO-H ($C_9H_{19}NO$): C, 68.74 (69.01); H, 12.18 (12.39); N, 8.91 (8.82). TEMPO-D was prepared analogously to TEMPO-H, using $(CD_3)_2CO/D_2O$ (99.9% D in D_2O) as the solvent; it was 98 ± 1% O*D* by NMR integration. Anal. Calcd (Found) for TEMPO-D ($C_9H_{18}DNO$): C, 68.30 (67.42); H, 12.10 (12.21); N, 8.85 (8.68). IR: ν_{OH}/ν_{OD} = 3495/2592 (CD_3CN), 3583/2648 (CD_2Cl_2), 3597/2658 (CCl_4).

Preparation of 4-MeO-TEMPO-H

A suspension of 4-MeO-TEMPO• (2.00 g, 10.7 mmol) and $Na_2S_2O_4$ (3.60 g, 20.7 mmol) in Me_2CO/H_2O (15 mL each) was stirred for 30 min at room temperature under N_2. The solvent was then partially evacuated under vacuum to remove Me_2CO. The leftover aqueous layer was extracted with Et_2O (3 × 20 mL), and the solvent was evacuated to dryness to give the crude product, which was purified by sublimation to a cold finger, yielding 951 mg of white powder (48%). ^{1}H NMR (CD_3CN): δ 1.09, 1.10 (s, CH_3, 6H each); 1.25, 1.90 (m, CH_2, 2H each); 3.25 (s, OCH_3, 3H); 3.46 (m, 4-CH, 1H); 5.37 (br s, OH, 1H). ^{1}H NMR (CD_2Cl_2): δ 1.16, 1.20 (s, CH_3, 6H each); 1.33, 1.90 (m, CH_2, 2H each); 3.32 (s, OCH_3, 3H); 3.44 (m, 4-CH, 1H); 4.51 (br s, OH, 1H). ^{13}C{^{1}H} NMR (CD_3CN): δ 20.83, 32.74 (CH_3); 45.25 (C3); 55.77 (OCH_3); 59.22 (C2); 72.57 (C4). ESI/MS$^+$: 188 $[M + H]^+$, 170 $[M – OH]^+$. Anal. Calcd (Found) for 4-MeO-TEMPO-H ($C_{10}H_{21}NO_2$): C, 64.13 (64.28); H, 11.30 (11.31); N, 7.48 (7.49). 4-MeO-TEMPO-D was prepared analogously using $(CD_3)_2CO/D_2O$ (99.9% D in D_2O) and was 98 ± 1% O*D* by NMR integration. Anal. Calcd (Found) for 4-MeO-TEMPO-D ($C_{10}H_{20}DNO_2$): C, 63.79 (63.92); H, 11.24 (11.37); N, 7.44 (7.55). IR (CD_3CN): ν_{OH}/ν_{OD} = 3492/2584.

^{1}H NMR Equilibrium Measurements

A typical experiment involved a J-Young sealable NMR tube being loaded with 4-oxo-TEMPO• (48 mg, 0.28 mmol) and TEMPO-H(D) (76 mg, 0.48 mmol) in 0.5 mL CD_3CN or CD_2Cl_2 to form an equilibrium mixture with 4-oxo-TEMPOH(D) and TEMPO•. ^{1}H NMR spectra of the sample were obtained at 278−318 K. All chemical species have resolvable peaks, whose integrations were determined by Lorentzian line fitting using NUTS.[25] An equilibrium constant was calculated at each temperature from the ratios of the peak areas, corrected for the number of protons for each peak. The experiment was repeated with 4-oxo-TEMPO•/TEMPO-H(D) = 32 mg/51 mg, and 24 mg/38 mg and the reported *K* at each temperature is the average of three runs. The errors on *K* are 2σ of the variation of measured values. The errors on ΔH^o and ΔS^o are 2σ errors from the least-squares linear fit using KaleidaGraph[59] to the Van't Hoff equation.

^{1}H NMR of TEMPO• in CD_3CN: −29.74 (3,5-CH_2, 4H), −16.51 (CH_3, 12H), 15.33 (4-CH_2, 2H); in CD_2Cl_2: −27.97 (3,5-CH_2, 4H), −15.14 (CH_3, 12H), 15.19 (4-CH_2, 2H). ^{1}H NMR of 4-oxo-TEMPO• in CD_3CN: −7.78 (CH_3, 12H), 1.80 (3,5-CH_2, broad, 4H, overlaps with residual solvent [CH_2DCN] peak); in CD_2Cl_2: −7.12 (CH_3, 12H), 2.22 (3,5-CH_2, 4H). ^{1}H NMR of 4-MeO-TEMPO• in CD_3CN: −33.89, −20.42 (3,5-CH_2, 2H each); −29.43, −1.74 (CH_3, 6H each); 3.07 (OCH_3, 3H); 8.67 (4-CH, 1H). ^{1}H NMR of ^{t}Bu$_2$NO• (s, ^{t}Bu) in CD_3CN: −6.67; in CD_2Cl_2: −6.20. 4-oxo-TEMPO-H and ^{t}Bu$_2$NOH were not isolated but were generated *in situ* in reactions 2 and 4, respectively. ^{1}H NMR of 4-oxo-TEMPO-H in CD_3CN: 1.22 (s, CH_3, 12H); 2.39 (s, CH_2, 4H); in CD_2Cl_2: 1.24 (s, CH_3, 12H); 2.49 (s, CH_2, 4H). ^{1}H NMR of ^{t}Bu$_2$NOH (s, ^{t}Bu) in CD_3CN: 1.23; in CD_2Cl_2: 1.31.

UV-Vis Stopped-Flow Kinetic Measurements

Solutions of 4-oxo-TEMPO$^{\bullet}$ (12−24 mM) and TEMPO-H(D) (118−584 mM) in MeCN or CH_2Cl_2 were prepared and loaded into gas-tight syringes inside a N_2 glovebox. The stopped-flow apparatus was flushed with the solvent, and a background spectrum was acquired. The syringes were immediately loaded onto the stopped-flow apparatus to minimize air exposure. The stopped-flow drive syringes were flushed with the reagents, then filled and allowed to thermally equilibrate. A minimum of six kinetic runs were performed for each set of concentrations at 278−318 K in MeCN or at 273−308 K in CH_2Cl_2 for reaction 2. The contents of the two syringes were rapidly mixed at equal volume resulting in half of the original concentrations (5.9−12 mM 4-oxo-TEMPO$^{\bullet}$ and 59−292 mM TEMPO-D). Kinetic data were analyzed using SPECFIT global analysis software[28] to determine the rate constants. Under pseudo-first order conditions (≥ 10 equiv TEMPO-H(D)), k_{obs} values were derived from fitting an A → B model at each [TEMPO-H(D)], and second order rate constants were obtained from plotting k_{obs} versus [TEMPO-H(D)] (Figure 3). Under second order conditions, the data were fit to an opposing second order equilibrium model, A + B ⇄ C + D (A and C colored), with a fixed equilibrium constant (Table 1). Reaction 2 was also performed in CCl_4 at 298 K under pseudo-first order conditions (≥ 10 equiv TEMPO-H(D)). Temperature dependent measurements of reaction 3 used similar amounts of 4-oxo-TEMPO$^{\bullet}$ and 4-MeOTEMPO-H (D) in MeCN; for reaction 4, 12−139 mM $^{t}Bu_2NO^{\bullet}$ and 118−237 mM TEMPO-H(D) in MeCN or CH_2Cl_2 were used (as the initial concentrations right after stopped-flow mixing). The errors on k are 2σ of the variation of measured values. The errors on the activation parameters are 2σ from the least-squares linear fit using KaleidaGraph[59] to the Eyring or Arrhenius equation.

Supplementary Material

Refer to Web version on PubMed Central for supplementary material.

Acknowledgments

We thank J. J. Warren for insightful discussions and the US National Institutes of Health (GM50422) and the University of Washington for financial support. The research at the University of North Texas was supported by the National Science and Robert A. Welch Foundations. Some of the results reported here were obtained on computers, purchased with funds provided by the National Science Foundation under grant CHE-0741936. E.A.M. gratefully acknowledges funding from the Natural Science and Engineering Research Council of Canada (NSERC PGS D2).

References

1. Hynes, JT.; Klinman, JP.; Limbach, H-H.; Schowen, RL., editors. Hydrogen-Transfer Reactions. Wiley-VCH; Weinheim: 2007.
2. a Hammes-Schiffer, S. Vol. 2. p. 479-502.b Fernandez-Ramos, A.; Ellingson, BA.; Garrett, BC.; Truhlar, DG. Reviews in Computational Chemistry. Cundari, TR.; Lipkowitz, KB., editors. Vol. 23. Wiley-VCH; Hoboken, NJ: 2007. p. 125-232. In ref. [1]
3. Bell, RP. The Tunnel Effect in Chemistry. Chapman and Hall; London: 1980. p. 77-105.
4. Carpenter, BK. Determination of Organic Reaction Mechanisms. John Wiley & Sons; 1984. p. 83-111.
5. cf a Klinman JP. Phil. Trans. R. Soc. B 2006;361:1323. [PubMed: 16873120] b Sutcliffe MJ, Masgrau L, Roujeinikova A, Johannissen LO, Hothi P, Basran J, Ranaghan KE, Mulholland AJ, Leys D, Scrutton NS. Phil. Trans. R. Soc. B 2006;361:1375. [PubMed: 16873125] c Barroso M, Arnaut LG, Formosinho SJ. J. Phys. Org. Chem 2009;22:254–263. d Meyer TJ, Huynh MHV. Inorg. Chem 2003;42:8140–8160. [PubMed: 14658865] e Reinaudt OM, Theopold KH. J. Am. Chem. Soc 1994;116:6979–6980. f Mahapatra S, Halfen JA, Tolman WB. J. Am. Chem. Soc 1996;118:11575–11586. g Zheng H, Lipscomb JD. Biochemistry 2006;45:1685–1692. [PubMed: 16460015]
6. Kochi, JK., editor. Free Radicals. Wiley; New York: 1973.
7. a Huynh MHV, Meyer TJ. Chem. Rev 2007;107:5004. [PubMed: 17999556] b Meyer TJ, Huynh MHV. Inorg. Chem 2003;42:8140. [PubMed: 14658865]c Hodgkiss, JM.; Rosenthal, J.; Nocera, DG.

Hydrogen-Transfer Reactions. Hynes, JT.; Klinman, JP.; Limbach, H-H.; Schowen, RL., editors. Vol. 2. Wiley-VCH; Weinheim: 2007. p. 503-562. d Stubbe J, Nocera DG, Yee CS, Chang MCY. Chem. Rev 2003;103:2167. [PubMed: 12797828] e Cukier RI, Nocera DG. Annu. Rev. Phys. Chem 1998;49:337. [PubMed: 9933908] f Partenheimer W. Catal. Today 1995;23:69.

8. a Mayer JM. Annu. Rev. Phys. Chem 2004;55:363. [PubMed: 15117257] b Mayer JM, Rhile IJ. Biochim. Biophys. Acta 2004;1655:51. [PubMed: 15100016] c Mayer JM, Rhile IJ, Larsen FB, Mader EA, Markle TF, DiPasquale AG. Photosynth. Res 2006;87:3. [PubMed: 16437185] d Mayer JM, Mader EA, Roth JP, Bryant JR, Matsuo T, Dehestani A, Bales BC, Watson EJ, Osako T, Valliant-Saunders K, Lam W-H, Hrovat DA, Borden WT, Davidson ER. J. Mol. Catal. A: Chem 2006;251:24.
9. a Knapp, MJ.; Meyer, M.; Klinman, JP. Hydrogen-Transfer Reactions. Hynes, JT.; Klinman, JP.; Limbach, H-H.; Schowen, RL., editors. Vol. 4. Wiley-VCH; Weinheim: 2007. p. 1241-1284. b Stubbe J, van der Donk WA. Chem. Rev 1998;98:705. [PubMed: 11848913]c Halliwell, B.; Gutteridge, JMC. Free Radicals in Biology and Medicine. Oxford University Press; Oxford: 1999.
10. a Knapp MJ, Rickert K, Klinman JP. J. Am. Chem. Soc 2002;124:3865. [PubMed: 11942823] b Lewis ER, Johansen E, Holman TR. J. Am. Chem. Soc 1999;121:1395.
11. Likhtenshtein, G.; Yamauchi, J.; Nakatsuji, S.; Smirnov, AI. Nitroxides: Applications in Chemistry, Biomedicine, and Materials Science. Wiley-VCH; New York: 2008.
12. a Sheldon RA, Arends IWCE. J. Mol. Catal. A: Chem 2006;251:200. b Sheldon RA, Arends IWCE. Adv. Synth. Catal 2004;346:1051. c Sheldon RA, Arends IWCE, Brink G-JT, Dijksman A. Acc. Chem. Res 2002;35:774. [PubMed: 12234207] d Vasbinder MJ, Bakac A. Inorg. Chem 2007;46:2322. [PubMed: 17298054] For other applications of nitroxyl radicals, see refs. [5-20] in
13. a Kreilick RW, Weissman SI. J. Am. Chem. Soc 1966;88:2645. b Arick MR, Weissman SI. J. Am. Chem. Soc 1968;90:1654. [PubMed: 4295237]
14. a Malievskii AD, Shapiro AB. Kinet. Catal 2005;46:472. b Malievskii AD, Koroteev SV, Shapiro AB. Kinet. Catal 2005;46:812. c Malievskii AD, Koroteev SV, Gorbunova NV, Brin EF. Kinet. Catal 1997;38:485.
15. Dijksman A, Marino-González A, Mairata i Payeras A, Arends IWCE, Sheldon RA. J. Am. Chem. Soc 2001;123:6826. [PubMed: 11448187]
16. Ishii Y, Sakaguchi S, Iwahama T. Adv. Synth. Catal 2001;343:393.
17. a Koshino N, Saha B, Espenson JH. J. Org. Chem 2003;68:9364. [PubMed: 14629158] b Koshino N, Cai Y, Espenson JH. J. Phys. Chem. A 2003;107:4262. c Amorati R, Lucarini M, Mugnaini V, Pedulli GF. J. Org. Chem 2003;68:1747. [PubMed: 12608787]
18. Cai Y, Koshino N, Saha B, Espenson JH. J. Org. Chem 2005;70:238. [PubMed: 15624928]
19. Roth JP, Yoder JC, Won T-J, Mayer JM. Science 2001;294:2524. [PubMed: 11752572]
20. Mader EA, Larsen AS, Mayer JM. J. Am. Chem. Soc 2004;126:8066. [PubMed: 15225018] H_2bip = 2,2′-bi-1,4,5,6-tetrahydropyrimidine.
21. Warren, JJ.; Mayer, JM. manuscript in preparation
22. a Ingold, KU.; In Kochi, JK., editors. Free Radicals. Vol. 1. Wiley; New York: 1973. p. 69ffb Russel, GA. Vol. 1. p. 275-331.c O'Neal, HE.; Benson, SW.; In Kochi, JK., editors. Free Radicals. Vol. 2. Wiley; New York: 1973. p. 302ff d Tedder JM. Angew. Chem. Int. Ed. Engl 1982;21:401. HAT rate constants have traditionally been analyzed using a correlation of Arrhenius activation energy E_a with enthalpic driving force ΔH (the Bell-Evans-Polanyi relation), together with ‘polar effects’ and other influences. In ref. [6]
23. a Mader EA, Davidson ER, Mayer JM. J. Am. Chem. Soc 2007;129:5153. [PubMed: 17402735] b Mader EA, Manner VW, Markle TF, Wu A, Franz JA, Mayer JM. J. Am. Chem. Soc 2009;131:4335–4345. [PubMed: 19275235]
24. a Wu A, Masland J, Swartz RD, Kaminsky W, Mayer JM. Inorg. Chem 2007;46:11190. [PubMed: 18052056] b Wu A, Mayer JM. J. Am. Chem. Soc 2008;130:14745–14754. [PubMed: 18841973] acac = 2,4-pentanedionato; py-imH = 2-(2′-pyridyl)imidazole.
25. NUTS – NMR Utility Transform Software, 1D version. Acorn NMR Inc.; Livermore, CA: 2003.
26. Bordwell FG, Liu W-Z. J. Am. Chem. Soc 1996;118:10819–10823. The close agreement between $\Delta G°_{4H}$ and the reported ΔBDE does not show that entropic effects are unimportant, since $\Delta S°(XOH) - \Delta S°(XO^{\bullet}) \cong 0$ is implicit in the Bordwell derivation of BDEs. For the bond dissociation free energy of TEMPO–H, and a discussion of entropies, see reference [23b].

27. Mader, EA. unpublished results The *CH* resonances for TEMPO-H broaden linearly with increasing $TEMPO^{\bullet}$ concentrations but the derived rate constants did not vary exponentially with temperature, suggesting that the self-exchange reaction is not the only source of the line broadening.
28. SPECFIT/32, versions v3.0.26 and v3.0.36. Spectrum Software Associates; Marlbourough, MA: 2000.
29. Sorokin A, Robert A, Meunier B. J. Am. Chem. Soc 1993;115:7293. The 'true' k_H/k_D, at complete deuteration, is equal to $\chi(D)/[(k_H/k_D)_{obs}^{-1} - \chi(H)]$, where $\chi(H)$ and $\chi(D)$ are the mole-fraction in H and D, respectively. For a discussion of the residual protio effect on the observed k_H/k_D, see
30. ΔBDE of 2,4,6-tri-*tert*-butylphenol (82.3 kcal mol^{-1}) and $^{t}Bu_2NOH$ (68.2 kcal mol^{-1}).[26]
31. Corchado, JC.; Chuang, Y-Y.; Coitino, EL.; Truhlar, DG. GAUSSRATE–version 9.5. University of Minnesota; Minneapolis, MN: 2007.
32. Frisch, MJ., et al. Gaussian 03, revision D.02. Gaussian, Inc.; Wallingford, CT: 2004.
33. Corchado, JC., et al. POLYRATE–version 9.5. University of Minnesota; Minneapolis, MN: 2007.
34. Lynch BJ, Fast PL, Harris M, Truhlar DG. J. Phys. Chem. A 2000;104:4811.
35. Zhao Y, Schultz NE, Truhlar DG. J. Chem. Theory Comput 2006;2:364–382.
36. Zhao Y, Truhlar DG. Theor. Chem. Accounts 2008;120:215–241.
37. a Frisch MJ, Pople JA, Binkley JS. J. Chem. Phys 1984;80:3265–3269. b Clark T, Chandrasekhar J, Spitznagel GW, Schleyer P. v. R. J. Comp. Chem 1983;4:294–301. c Hehre WJ, Ditchfield R, Pople JA. J. Chem. Phys 1972;56:2257–2261.
38. Fernandez-Ramos, A.; Ellingson, BA.; Garrett, BC.; Truhlar, DG. Reviews in Computational Chemistry. Lipkowitz, KB.; Cundari, TR., editors. Vol. 23. Wiley-VCH; Hoboken, NJ: 2007. p. 125-232.
39. Shelton GR, Hrovat DA, Borden WT. J. Am. Chem. Soc 2007;129:164. [PubMed: 17199295] When the tunneling distance is large, there is a temperature range in which D tunnels considerably closer to the top of the barrier than H, so that the probability of passing through or over the barrier is actually greater for D than for H. As a result, in this temperature range, $E_{a,D} - E_{a,H} > 1.3$ kcal/mol, but $\log(A_H/A_D) < 0$. See, for example
40. a Mayer JM, Hrovat DA, Thomas JL, Borden WT. J. Am. Chem. Soc 2002;124:11142–11147. [PubMed: 12224962] b Litwinienko G, Ingold KU. Acc. Chem. Res 2007;40:222–230. [PubMed: 17370994] c Waidmann CR, Zhou X, Tsai EA, Kaminsky W, Hrovat DA, Borden WT, Mayer JM. J. Am. Chem. Soc 2009;131:4729–4743. [PubMed: 19292442]In some circumstances, it is valuable to distinguish between an 'HAT mechanism' where the e^- and H^+ come from/transfer to the same bond, vs. a 'PCET mechanism' in which the two particles are separated in the reactants and/or products. See the discussion in
41. Roth JP, Lovell S, Mayer JM. J. Am. Chem. Soc 2000;122:5486.
42. b Mori Y, Sakaguchi Y, Hayashi H. J. Phys. Chem. A 2000;104:4896. c Semmelhack MF, Chou CS, Cortes DA. J. Am. Chem. Soc 1983;105:4492–4494. e Chantooni MK Jr. Kolthoff IM. J. Phys. Chem 1976;80:1306–1310. (a) $\Delta G°(ET) = -23.1[E(TEMPO^{\bullet}) - E(TEMPO\text{-}H)] \approx 60$ kcal mol^{-1}. $\Delta G°(PT) = -1.37[pK_a(TEMPO\text{-}H^{\bullet+}) - pK_a(TEMPO\text{-}H)] = \Delta G°(ET)$. $E(TEMPO^{\bullet}) \approx -1.91$ V versus $Cp_2Fe^{+/0}$: $E(TEMPO\text{-}H) \approx 0.71$ V versus $Cp_2Fe^{+/0}$: (d) $pK_a(TEMPO\text{-}H) \approx 41$ in MeCN is estimated from $pK_a(TEMPO\text{-}H) = 31.0$ in DMSO.26 pK_a conversion from DMSO to MeCN: (f) $pK_a(TEMPO\text{-}H^{\bullet+}) = pK_a(TEMPO\text{-}H) + 23.1[E(TEMPO^{\bullet}) - E(TEMPO\text{-}H)]/1.37 \approx -3$.
43. a Avila DV, Ingold KU, Lusztyk J, Green WH, Procopio DR. J. Am. Chem. Soc 1995;117:2929–30. b Valgimigli L, Banks JT, Ingold KU, Lusztyk J. J. Am. Chem. Soc 1995;117:9966–71. c Snelgrove DW, Lusztyk J, Banks JT, Mulder P, Ingold KU. J. Am. Chem. Soc 2001;123:469–477.
44. b Abraham MH, Grellier PL, Prior DV, Morris JJ, Taylor PJ. J. Chem. Soc., Perkin Trans. 2 1990:521. c Abraham MH, Grellier PL, Prior DV, Duce PP, Morris JJ, Taylor PJ. J. Chem. Soc., Perkin Trans. 2 1989:699.d Warren, JJ. unpublished results (a) In the Litwinienko/Ingold/Abraham model,[43, 44b,c] the CH_2Cl_2/MeCN kinetic solvent effect is given by $\log(k_{CH2Cl2}/k_{MeCN}) = 8.3\alpha_2^{H}(\beta_2^{H}{}_{MeCN} - \beta_2^{H}{}_{CH2Cl2})$. Using α_2^{H} (the solute constant) = 0.29 for dialkylhydroxylamines and β_2^{H} (the hydrogen-bond acceptor solvent constant) = 0.44 for MeCN and 0.05 for CH_2Cl_2,[45] this model predicts $k_{CH2Cl2}/k_{MeCN} = 8.7$, in modest agreement with the experimental values of 4.8 ± 0.6 and 2.4 ± 0.3 for reactions 2 and 4. However, in our experience[44e] this model is not very accurate for reactions in CH_2Cl_2 (see reference [45]). The Ingold/Abraham model may be incomplete for this

example because the interaction of TEMPO ($\beta_2^H = 0.46$) with CH_2Cl_2 ($\alpha_2^H = 0.15$) may be as important as the interaction of TEMPOH with CH_2Cl_2. The radical-solvent interaction is absent in many radical reactions because α_2^H(solvent) or β_2^H(RO•) is negligible.

45. b Galian RE, Litwinienko G, Pérez-Prieto J, Ingold KU. J. Am. Chem. Soc 2007;129:9280–9281. [PubMed: 17625849] c Foti MC, Daquino C, Mackie ID, DiLabio GA, Ingold KU. J. Org. Chem 2008;73:9270–9282. (a) The β_2^H is given as 0.05 for CH_2Cl_2 by Abraham et al.[44b,c] A different value of 0.15 has been suggested using the KSE model,[45b] which was later revised to 0.20.[45c] As pointed out by a reviewer, the agreement with the KSE model is better using these revised values. However, we feel that the KSE model becomes more circular and less valuable when the β_2^H values are not independent parameters but rather extracted from the radical reaction rates.
46. a Knauer BR, Napier JJ. J. Am. Chem. Soc 1976;98:4395–4400. b Improta R, Barone V. Chem. Rev 2004;104:1231–1254. [PubMed: 15008622]
47. Beckwith ALJ, Bowry VW, Ingold KU. J. Am. Chem. Soc 1992;114:4983–4992.
48. The experimental difference in zero-point energies for TEMPO-H(D) in MeCN is estimated as 0.5 $[\nu_{OH} - \nu_{OD}] = 452\ cm^{-1} = 1.3\ kcal\ mol^{-1}$.
49. Horng ML, Gardecki JA, Papazyan A, Maroncelli M. J. Phys. Chem 1995;99:17311. The KIEs are not sensitive to solvent even though the characteristic solvent reorganization times are about a factor of two longer for CH_2Cl_2 than for MeCN:
50. a Cotton FA, Felthouse TR. Inorg. Chem 1982;21:2667. b Andersen B, Andersen P. Acta Chem. Scand 1966;20:2728. c Bordeaux PD. Acta Crystallogr., Sect. B 1974;30:790. (a) $^tBu_2NO^•$ is slightly more crowded than the cyclic analogs, as reflected in its slightly larger CNC angle of 129.6(3)° versus 123.5(2)° for 4-oxo-TEMPO$^•$. Two molecules of $^tBu_2NO^•$ were co-crystallized with $Rh_2(O_2CCF_3)_4(H_2O)_2$. ∠CNC = 136(3)° of $^tBu_2NO^•$ in the gas phase was determined by electron diffraction.
51. a Cape JL, Bowman MK, Kramer DM. J. Am. Chem. Soc 2005;127:4208. [PubMed: 15783202] b Ludlow MK, Soudackov AV, Hammes-Schiffer S. J. Am. Chem. Soc 2009;131:7094–7102. [PubMed: 19351186] c Yoder JC, Roth JP, Gussenhoven EM, Larsen AS, Mayer JM. J. Am. Chem. Soc 2003;125:2629. [PubMed: 12603151] $E_{aD} - E_{aH} = -2.8\ kcal\ mol^{-1}$ and $\log(A_H/A_D) = 2.2$ have been reported for e^-/H^+ from 2,3-dimethoxy-5-methyl-1,4-benzoquinol to the excited state of [Ru(2,2′-bipyridine)$_2${2-(2-pyridyl)benzimidazolate}$^+$]: This result has very recently been rationalized in terms of being close to the Marcus inverted region for PCET: HAT self-exchange between $[Fe^{II}(H_2bip)_3]^{2+}$ and $[Fe^{III}(H_2bip)_2(Hbip)]^{2+}$ (H_2bip = 2,2'-bi-1,4,5,6-tetrahydropyrimidine) also appears to have negative $E_{aD} - E_{aH} = -1.2 \pm 0.8\ kcal\ mol^{-1}$ and positive $\log(A_H/A_D) = 0.9 \pm 1.2$ values:
52. Foti M, Ingold KU, Lusztyk J. J. Am. Chem. Soc 1994;116:9440.
53. Mendenhall GD, Ingold KU. J. Am. Chem. Soc 1973;95:627–628.
54. Chenier JHB, Howard JA. Can. J. Chem 1975;53:623.
55. Griller D, Ingold KU. J. Am. Chem. Soc 1974;96:630.
56. Bordwell FG, Cheng J. J. Am. Chem. Soc 1991;113:1736.
57. a Doba T, Ingold KU. J. Am. Chem. Soc 1984;106:3958. b Malatesta V, Ingold KU. J. Am. Chem. Soc 1981;103:3094.
58. Ozinskas AJ, Bobst AM. Helv. Chim. Acta 1980;63:1407.
59. KaleidaGraph, version 3.5. Synergy Software; 2000.

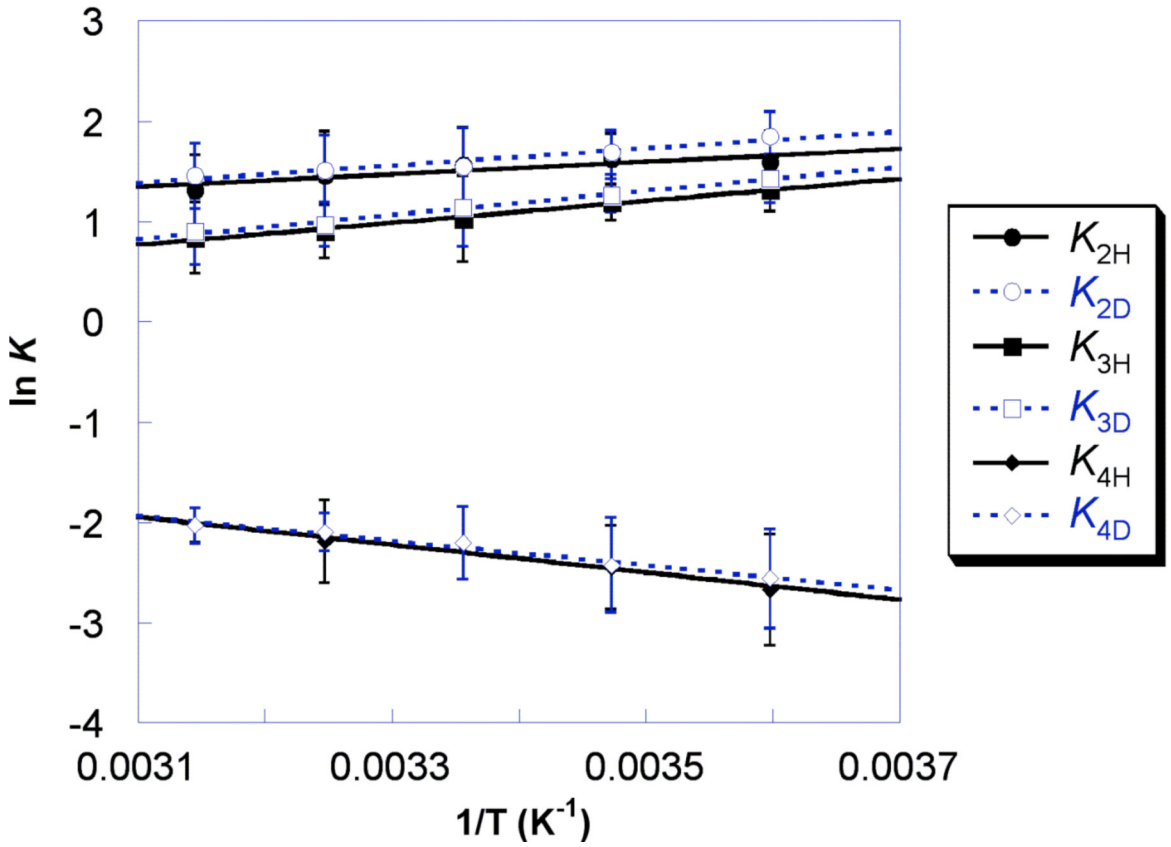

Figure 1.
Van't Hoff plot for reactions 2−4 in CD_3CN at 278−318 K.

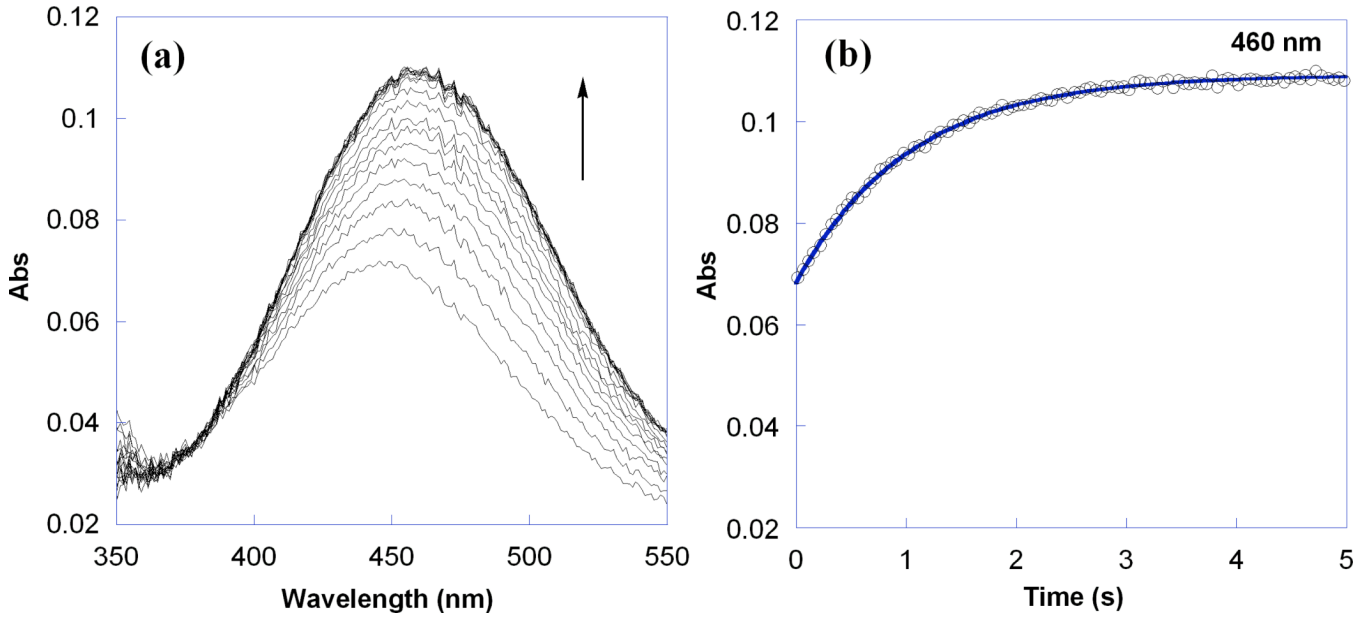

Figure 2.
(a) Overlay of UV-vis spectra for the reaction of 8.8 mM 4-oxo-TEMPO$^{\bullet}$ with 88 mM TEMPO-H (eq 2) in MeCN over 5 s at 298 K. (b) Absorbance at 460 nm showing the raw data (○) and first order A → B fit using SPECFIT (—).

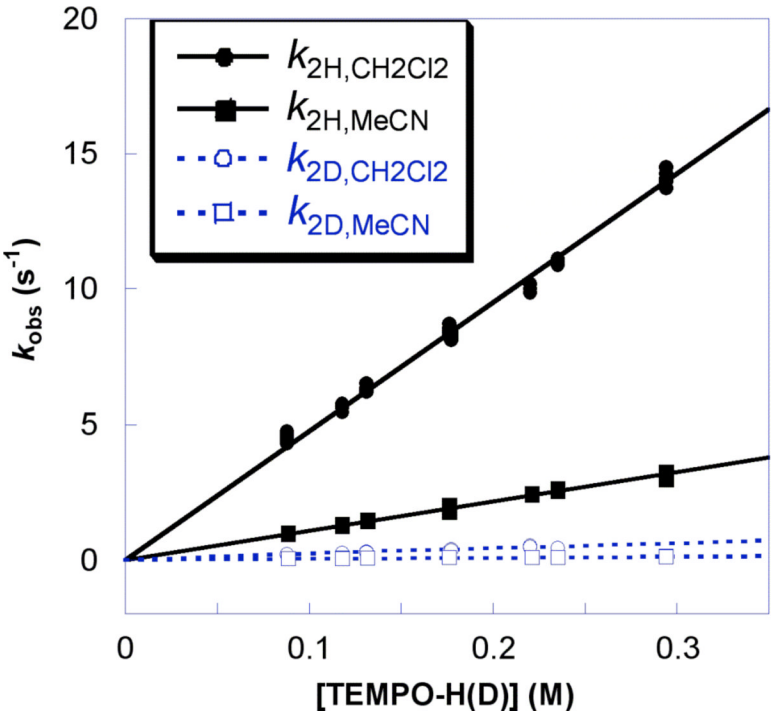

Figure 3.
Plot of pseudo first order k_{obs} versus [TEMPO-H(D)] for reaction 2 in MeCN (k_H/k_D = 23 ± 3) and in CH_2Cl_2 (k_H/k_D = 23 ± 4) at 298 K.

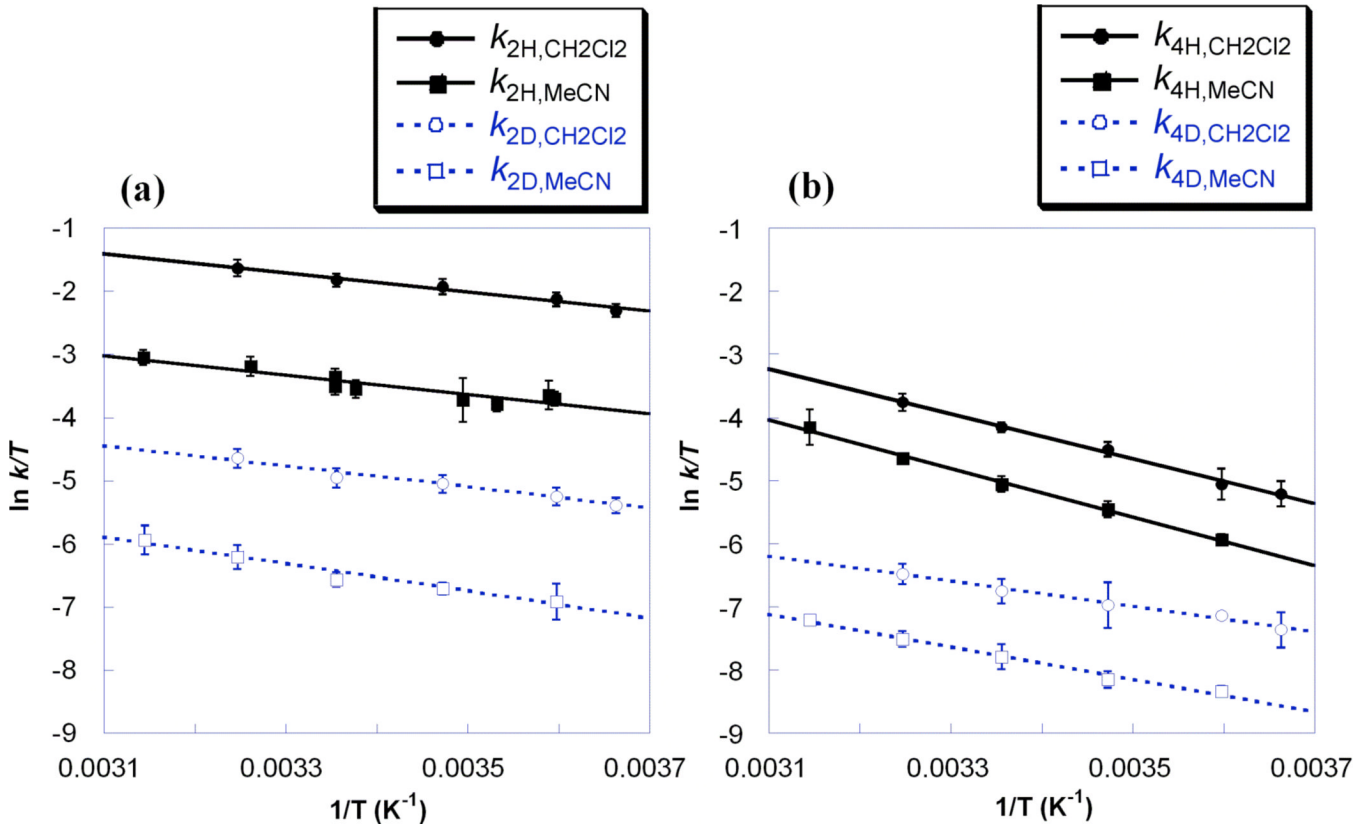

Figure 4.
Eyring plots for (a) 4-oxo-TEMPO$^{\bullet}$ + TEMPO-H (reaction 2) and (b) $^{t}Bu_2NO^{\bullet}$ + TEMPO-H (reaction 4), both in MeCN and CH_2Cl_2.

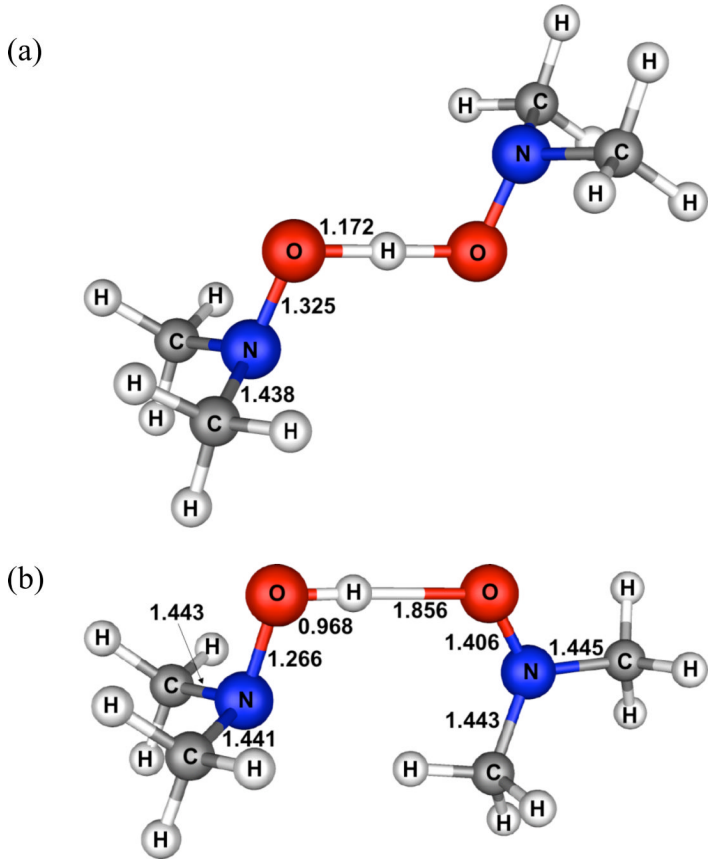

Figure 5.
(a) Transition structure for hydrogen transfer between $(CH_3)_2NOH$ and $(CH_3)_2NO^{\bullet}$. (b) H-bonded complex between $(CH_3)_2NOH$ and $(CH_3)_2NO^{\bullet}$. Bond lengths are in Ångstroms.

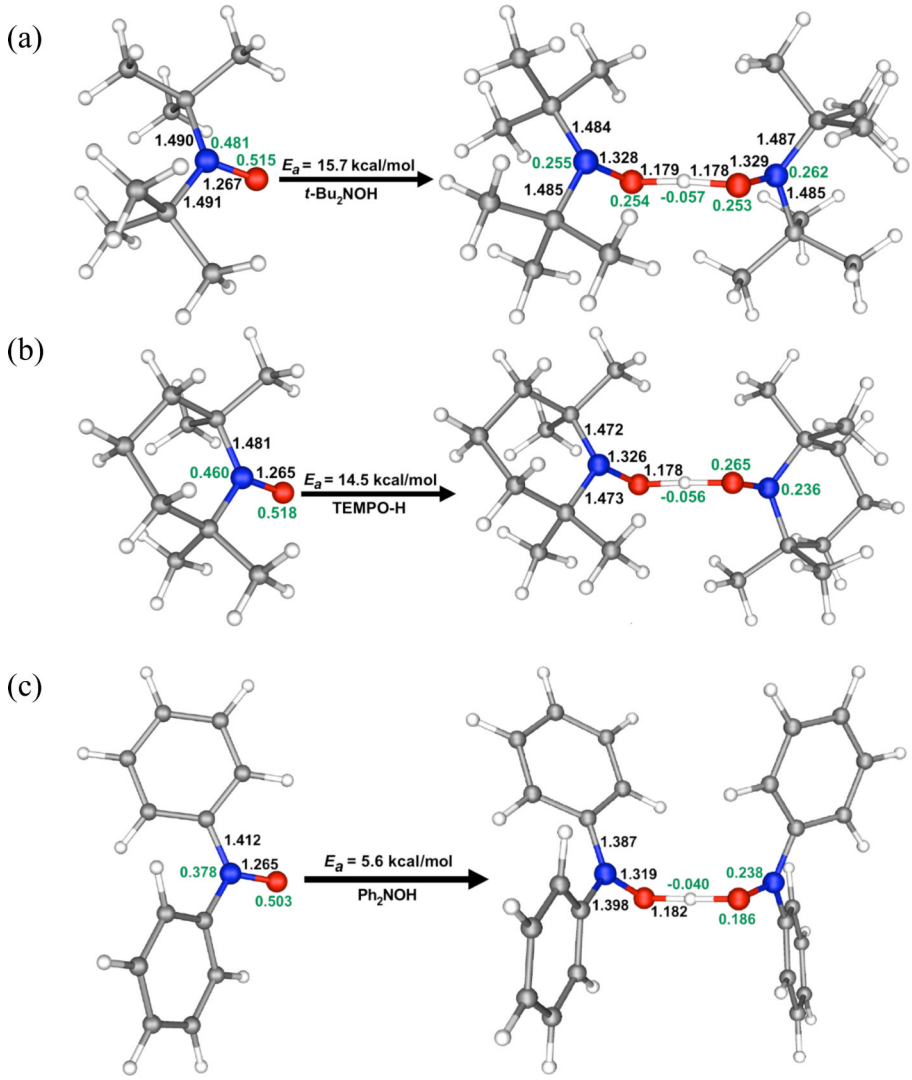

Figure 6.

Bond lengths (Å), atomic spin densities (in green), and activation energies (kcal mol^{-1}) for the nitroxyl radicals, (a) ^{t}Bu$_2$NO$^\bullet$, (b) TEMPO$^\bullet$, and (c) Ph$_2$NO$^\bullet$, and the transition structures and CVT activation energies for their hydrogen self-exchange reactions with the corresponding hydroxylamines.

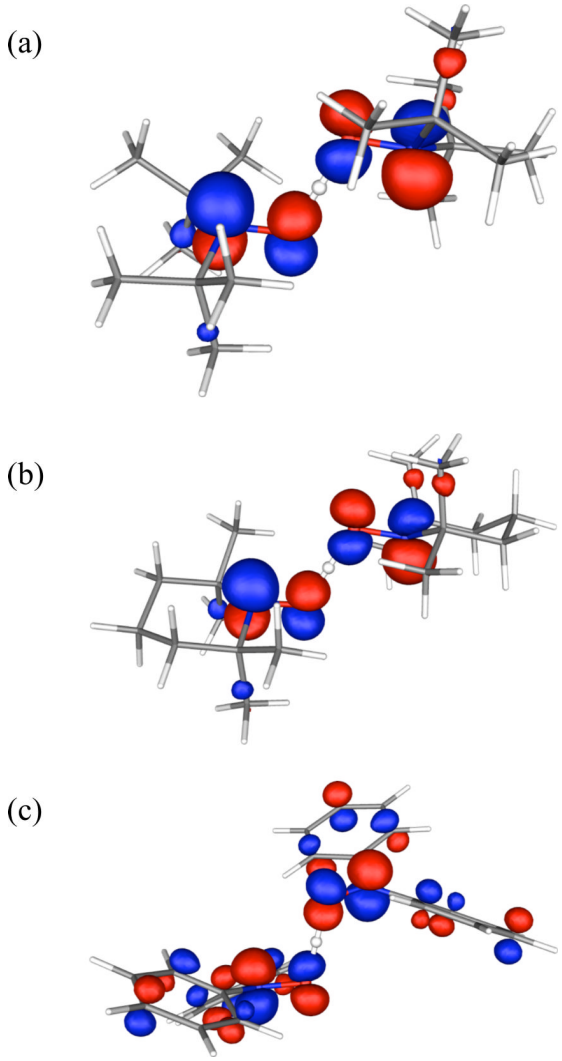

Figure 7.
SOMOs of the transition structures for hydrogen exchange reactions: (a) $^{t}Bu_2NO^{\bullet}$ + $^{t}Bu_2NOH$, (b) TEMPO$^{\bullet}$ + TEMPO-H , and (c) $Ph_2NO^{\bullet}$ + Ph_2NOH.

Table 1

Thermodynamic Parameters for Pseudo Self-Exchange Reactions of Nitroxyl Radicals and Hydroxylamines.[a]

Reaction	Solvent	*K* (298 K)	Δ*H*°	Δ*S*°
(2) 4-oxo-TEMPO$^{\bullet}$ + TEMPO-H	CD_3CN	4.5 ± 1.8	−1.7 ± 0.7	−2.6 ± 2.1
4-oxo-TEMPO$^{\bullet}$ + TEMPO-D	CD_3CN	4.7 ± 1.8	−1.7 ± 0.7	−2.5 ± 2.4
4-oxo-TEMPO$^{\bullet}$ + TEMPO-H	CD_2Cl_2	7.6 ± 2.4	−2.6 ± 0.8	−4.8 ± 2.6
4-oxo-TEMPO$^{\bullet}$ + TEMPO-D	CD_2Cl_2	6.6 ± 2.2	−2.6 ± 0.8	−5.1 ± 2.8
(3) 4-oxo-TEMPO$^{\bullet}$ + 4-MeO-TEMPO-H	CD_3CN	2.8 ± 1.2	−2.2 ± 0.4	−5.8 ± 2.3
4-oxo-TEMPO$^{\bullet}$ + 4-MeO-TEMPO-D	CD_3CN	3.1 ± 1.2	−2.4 ± 0.7	−5.8 ± 2.3
(4) $^{t}Bu_2NO^{\bullet}$ + TEMPO-H	CD_3CN	0.11 ± 0.02	2.7 ± 0.9	4.6 ± 2.8
$^{t}Bu_2NO^{\bullet}$ + TEMPO-D	CD_3CN	0.11 ± 0.03	2.4 ± 0.9	3.7 ± 2.9
$^{t}Bu_2NO^{\bullet}$ + TEMPO-H	CD_2Cl_2	0.10 ± 0.02	3.1 ± 0.8	5.6 ± 2.6
$^{t}Bu_2NO^{\bullet}$ + TEMPO-D	CD_2Cl_2	0.10 ± 0.02	3.1 ± 0.8	5.8 ± 2.4

[a] Measurements at 278−318 K; Δ*H*° in kcal mol^{-1}, Δ*S*° in cal mol^{-1} K^{-1}.

Table 2

Driving Forces, Rate Constants, and Kinetic Isotope Effects for Nitroxyl plus Hydroxylamine Reactions.[a]

Reaction	Solvent	$\Delta G°^{b}$	k_H (M^{-1} s^{-1})[a]	k_D (M^{-1} s^{-1})[a,c]	k_H/k_D[a,c]	Ref.
4-oxo-TEMPO$^{\bullet}$ + TEMPO-H[d]	MeCN	−0.9 ± 0.2	10 ± 1	0.44 ± 0.05	23 ± 3	*e*
4-oxo-TEMPO$^{\bullet}$ + TEMPO-H	CH_2Cl_2	−1.2 ± 0.2	48 ± 4	2.1 ± 0.3	23 ± 4	*e*
4-oxo-TEMPO$^{\bullet}$ + TEMPO-H	CCl_4	–	300 ± 30	17 ± 4	18 ± 5	*e*
4-oxo-TEMPO$^{\bullet}$ + 4-MeO-TEMPO-H	MeCN	−0.6 ± 0.2	7.8 ± 0.7	0.37 ± 0.05	21 ± 3	*e*
$^{t}Bu_2NO^{\bullet}$ + TEMPO-H	MeCN	1.3 ± 0.2	1.9 ± 0.2	0.12 ± 0.02	16 ± 3	*e*
$^{t}Bu_2NO^{\bullet}$ + TEMPO-H	CH_2Cl_2	1.4 ± 0.2	4.6 ± 0.4	0.35 ± 0.04	13 ± 2	*e*
PINO$^{\bullet}$ + 4Me-NHPI[f]	AcOH(D)	−0.4 ± 0.1	677 ± 24	61.3 ± 2.1	11.0 ± 0.5	18
4-Me-PINO$^{\bullet}$ + NHPI[f]	AcOH(D)	0.4 ± 0.1	354 ± 23	31.8 ± 2.0	11.1 ± 1.0	18
$^{t}Bu_2NO^{\bullet}$ + $^{t}Bu_2NOH$	CCl_4	0	320 ± 40	–	–	13
$^{t}Bu_2NO^{\bullet}$ + $^{t}Bu_2NOH$	C_6H_5Cl	0	240 ± 60	–	–	13
$^{t}Bu(Ar)NO^{\bullet}$ + $^{t}Bu(Ar)NOH$[g]	CCl_4	0	$(2.0 \pm 0.4) \times 10^3$	$(1.3 \pm 0.2) \times 10^3$	1.5 ± 0.4	13
$^{t}Bu(Ar)NO^{\bullet}$ + $^{t}Bu(Ar)NOH$[g]	C_6H_5Cl	0	$(5.2 \pm 0.4) \times 10^2$	–	–	13
$^{t}Bu(Ar)NO^{\bullet}$ + $^{t}Bu(Ar)NOH$[g]	CH_2Cl_2	0	< 20	–	–	13
$Ph_2NO^{\bullet}$ + Ph_2NOH	CCl_4	0	$> 10^7$	–	–	13
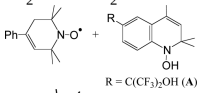	hexane	−0.2 ± 0.1	$(4.3 \pm 0.2) \times 10^4$	$(2.5 \pm 0.1) \times 10^4$	1.7 ± 0.1	14
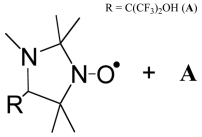	hexane	2.0 ± 0.1	$(4.5 \pm 0.2) \times 10^3$	$(2.9 \pm 0.2) \times 10^3$	1.6 ± 0.1	14
B + **A** (R = CPh_3)	hexane	0.9 ± 0.1	$(1.4 \pm 0.1) \times 10^4$	$(7.3 \pm 0.4) \times 10^3$	1.9 ± 0.2	14
B (R = Ph) + **A**	hexane	1.6 ± 0.1	$(8.6 \pm 0.4) \times 10^3$	$(5.7 \pm 0.3) \times 10^3$	1.5 ± 0.1	14
TEMPO$^{\bullet}$ + **A**	hexane	−0.6 ± 0.1	$(7.6 \pm 0.4) \times 10^4$	–	–	14
TEMPO$^{\bullet}$ + **A** (R = CPh_3)	hexane	−1.4 ± 0.1	$(1.5 \pm 0.1) \times 10^5$	–	–	14
4-oxo-TEMPO$^{\bullet}$ + **A**	hexane	−1.3 ± 0.1	$(6.4 \pm 0.3) \times 10^4$	–	–	14

[a] T = 298 (this work and ref.[18]), 300 (ref. [13]), and 293 K (ref. [14]); – means not determined.

[b] kcal mol^{-1}.

[c] Not corrected for the incomplete (98±1%) deuterium enrichment; the true k_H/k_D values are roughly a factor of two higher; see text.

[d] Ref. 20.

[e] This work.

[f] PINO$^{\bullet}$ = phthalimide *N*-oxyl radical, NHPI = *N*-hydroxyphthalimide.

[g] Ar = 2,6-dimethoxyphenyl.

Table 3

Eyring and Arrhenius Parameters for H- and D-Atom Transfer Reactions.[a]

Reaction	Solvent	T (K)	$\Delta H^{\ddagger}$	$\Delta S^{\ddagger}$	E_a	log A
4-oxo-TEMPO$^{\bullet}$ + TEMPO-H[b]	MeCN	278−318	3.0 ± 0.5	−43 ± 3	3.6 ± 0.5	3.8 ± 0.6
4-oxo-TEMPO$^{\bullet}$ + TEMPO-D	MeCN	278−318	4.3 ± 0.4	−46 ± 2	4.9 ± 0.4	3.3 ± 0.4
4-oxo-TEMPO$^{\bullet}$ + TEMPO-H	CH_2Cl_2	273−308	3.0 ± 0.4	−41 ± 2	3.6 ± 0.4	4.3 ± 0.4
4-oxo-TEMPO$^{\bullet}$ + TEMPO-D	CH_2Cl_2	273−308	3.3 ± 0.4	−46 ± 2	3.9 ± 0.4	3.2 ± 0.4
4-oxo-TEMPO$^{\bullet}$ + 4-MeO-TEMPO-H	MeCN	278−318	4.8 ± 0.3	−38 ± 2	5.4 ± 0.3	4.9 ± 0.4
4-oxo-TEMPO$^{\bullet}$ + 4-MeO-TEMPO-D	MeCN	288−328	5.4 ± 0.3	−42 ± 2	6.0 ± 0.3	4.0 ± 0.4
$^{t}Bu_2NO^{\bullet}$ + TEMPO-H	MeCN	278−318	7.7 ± 0.3	−31 ± 2	8.3 ± 0.3	6.4 ± 0.4
$^{t}Bu_2NO^{\bullet}$ + TEMPO-D	MeCN	278−318	5.1 ± 0.3	−45 ± 2	5.7 ± 0.3	3.3 ± 0.4
$^{t}Bu_2NO^{\bullet}$ + TEMPO-H	CH_2Cl_2	273−308	7.1 ± 0.3	−32 ± 2	7.6 ± 0.3	6.3 ± 0.4
$^{t}Bu_2NO^{\bullet}$ + TEMPO-D	CH_2Cl_2	273−308	4.0 ± 0.3	−47 ± 2	4.5 ± 0.3	2.9 ± 0.4
PINO$^{\bullet}$ + 4Me-NHPI[c]	AcOH	290−309	9.8 ± 0.2	−13 ± 1	10.4 ± 0.2	10.4 ± 0.2
4-Me-PINO$^{\bullet}$ + NHPI[c]	AcOH	290−309	10.0 ± 0.2	−13 ± 1	10.6 ± 0.2	10.4 ± 0.2

[a] $\Delta H^{\ddagger}$, E_a in kcal mol^{-1}; $\Delta S^{\ddagger}$ in cal mol^{-1} K^{-1}.

[b] Originally reported in ref. 20.

[c] Ref. 18.

Table 4

Kinetic Isotope Effects and Differences in Protio and Deutero Arrhenius Parameters.[a]

Reaction	solvent	k_H/k_D	$E_{aD} - E_{aH}$	$\log(A_H/A_D)$
4-oxo-TEMPO$^{\bullet}$ + TEMPO-H	MeCN	23 ± 3	1.3 ± 0.6	0.5 ± 0.7
4-oxo-TEMPO$^{\bullet}$ + TEMPO-H	CH_2Cl_2	23 ± 4	0.3 ± 0.6	1.1 ± 0.6
4-oxo-TEMPO$^{\bullet}$ + 4-MeO-TEMPO-H	MeCN	21 ± 3	0.6 ± 0.4	0.9 ± 0.6
$^{t}Bu_2NO^{\bullet}$ + TEMPO-H	MeCN	16 ± 3	−2.6 ± 0.4	3.1 ± 0.6
$^{t}Bu_2NO^{\bullet}$ + TEMPO-H	CH_2Cl_2	13 ± 2	−3.1 ± 0.4	3.4 ± 0.6

[a] k_H/k_D at 298 K, $E_{aD} - E_{aH}$ in kcal mol^{-1}.

Table 5

Computed canonical variational transition state theory (CVT) and small curvature tunneling (SCT) rate constants and Arrhenius activation parameters for at the MPW1K/6−31+G(d,p) level of theory.

Reaction	Method	k_H	k_D	k_H/k_D	$E_{a,H}$	log(A_H)	$E_{a,D}$	log(A_D)
$Me_2NO^{\bullet}$ + $HONMe_2$	CVT	5.65×10^{-4}	8.67×10^{-5}	6.5	14.8	7.6	15.8	7.6
$Me_2NO^{\bullet}$ + $HONMe_2$	SCT	4.85×10^{1}	2.47×10^{-1}	196	6.1	6.2	7.3	4.8
$MeHNO^{\bullet}$ + HONHMe	SCT	1.83×10^{1}	7.65×10^{-2}	239	6.1	5.8	7.4	4.3

[a] k_H, k_D, M^{-1} s^{-1}; $E_{a,H}$, $E_{a,D}$, kcal mol^{-1}.